Quaternary Science Reviews xxx (2013) 1–18

Contents lists available at SciVerse ScienceDirect

Quaternary Science Reviews

journal homepage: www.elsevier.com/locate/quascirev

Neoglacial change in deep water exchange and increase of sea-ice transport through eastern Fram Strait: evidence from radiogenic isotopes

Kirstin Werner [a,*], Martin Frank [a], Claudia Teschner [a], Juliane Müller [b], Robert F. Spielhagen [a,c]

[a] GEOMAR Helmholtz Centre for Ocean Research Kiel, Wischhofstraße 1-3, 24148 Kiel, Germany
[b] Alfred Wegener Institute for Polar and Marine Research, Telegrafenberg A5, 14473 Potsdam, Germany
[c] Academy of Sciences, Humanities, and Literature Mainz, Geschwister-Scholl-Straße 2, 55131 Mainz, Germany

ARTICLE INFO

Article history:
Received 11 January 2013
Received in revised form
6 June 2013
Accepted 14 June 2013
Available online xxx

Keywords:
Holocene
Radiogenic isotopes
Neodymium
Arctic
Fram Strait
Multiproxy study

ABSTRACT

Sediment core MSM5/5-712 from the West Spitsbergen continental margin has been investigated at high resolution for its seawater-derived neodymium (Nd) and lead (Pb) isotope compositions stored in ferromanganese oxyhydroxide coatings of the sediment particles to reconstruct Holocene changes in the sources and mixing of bottom waters passing the site. The radiogenic isotope data are used in combination with a multitude of proxy indicators for the climatic and oceanographic development of the eastern Fram Strait during the past 8500 years. To calibrate the downcore data, seawater and core top samples from the area were analysed for their radiogenic isotope compositions. Core top leachates reveal relatively high (more radiogenic) Nd isotope compositions between ε_{Nd} −9.7 and −9.1, which are higher than present-day seawater ε_{Nd} in eastern Fram Strait (−12.6 to −10.5) and indicate that the seawater values have only been established very recently. The core top data agree well with the downcore signatures within the uppermost 40 cm of the sediment core (ε_{Nd} −9.1 to −8.8) indicating a reduced inflow of waters from the Nordic Seas, concurrent with cool conditions and a south-eastward shift of the marginal ice zone after ca 2.8 cal ka BP (Late Holocene). High sea-ice abundances in eastern Fram Strait are coeval with the well-known Neoglacial trend in the northern North Atlantic region. In contrast, warmer conditions of the late Early to Mid-Holocene were accompanied by lower (less radiogenic) ε_{Nd} signatures of the bottom waters indicating an increased admixture from the Nordic Seas (−10.6 to −10.1).

A shift to significantly more radiogenic ε_{Nd} signatures of the detrital material also occurred at 3 cal ka BP and was accompanied by a marked increase in supply of fine-grained ice-rafted material (IRF) from the Arctic Ocean to the core site. The most likely source areas for this radiogenic material are the shallow Arctic shelves, in particular the Kara Sea shelf.

The evolution of the Pb isotope compositions of past seawater was dominated by local signatures characterized by high $^{208,\ 207,\ 206}Pb/^{204}Pb$ values during the warm Early and Mid-Holocene periods related to enhanced chemical weathering on Svalbard and high glacial and riverine input derived from young granitic (more radiogenic) material to the West Spitsbergen margin. At 3 cal ka BP both detrital and seawater Pb isotope data changed towards more Kara Sea-like signatures.

1. Introduction

The Fram Strait is the only deepwater connection of the Arctic Ocean to the world's oceans (Fig. 1). It plays a major role for the transport of heat to the Arctic (Rudels et al., 2000; Karcher et al., 2003; Schauer et al., 2004) and also controls freshening of the Nordic Seas through Arctic sea-ice export (Mauritzen and Häkkinen, 1997). It is the location where warm and saline Atlantic Water (AW) either returns to the North Atlantic within the Fram Strait as the Return Atlantic Current (RAC; 200–300 m depth) or enters the Arctic Ocean, crosses the Arctic basin and flows back into the North Atlantic through western Fram Strait where it mixes with the RAC at water depths up to 500 m (Rudels et al., 2005). In this way a substantial part of cooled, high-salinity AW masses (Arctic

* Corresponding author.
E-mail addresses: kwerner@geomar.de, kirstinwerner@gmx.de (K. Werner).

0277-3791/$ – see front matter © 2013 Elsevier Ltd. All rights reserved.
http://dx.doi.org/10.1016/j.quascirev.2013.06.015

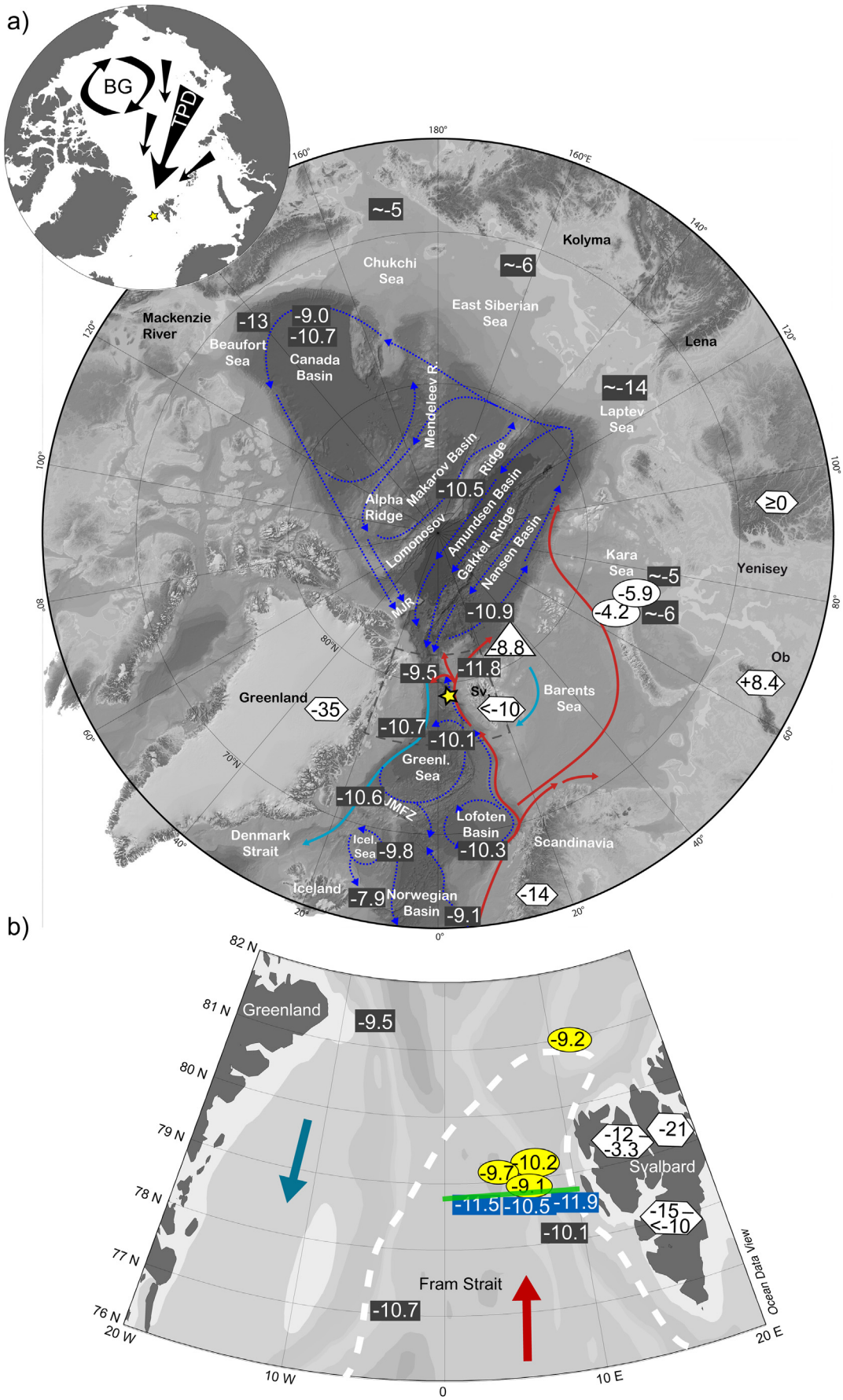

Please cite this article in press as: Werner, K., et al., Neoglacial change in deep water exchange and increase of sea-ice transport through eastern Fram Strait: evidence from radiogenic isotopes, Quaternary Science Reviews (2013), http://dx.doi.org/10.1016/j.quascirev.2013.06.015

Intermediate Water, AIW) are provided to join the East Greenland Current (EGC) in the western Fram Strait thereby contributing to deepwater renewal processes in the Nordic Seas (Mauritzen, 1996; Anderson et al., 1999; Rudels et al., 1999). Thermohaline convection processes in the Nordic Seas which strongly influence the present-day climate system (Broecker, 1991) are further controlled by the extent of Arctic sea ice. Arctic sea-ice coverage not only governs atmospheric and surface ocean temperatures through its albedo and insulating effects but after export via Fram Strait also supplies freshwater to the regions of thermohaline convection and deep-water formation in the Nordic Seas (Mauritzen and Häkkinen, 1997; Lohmann and Gerdes, 1998; Holland et al., 2001).

Deepwater flow and its decadal variability in the eastern Fram Strait and the Arctic Ocean are still a matter of debate (Jones, 2001). The contributions of different water masses to the deeper parts of the West Spitsbergen Current (WSC) are as yet not completely understood. Studies carried out since the 1980s by e.g., Aagaard et al. (1985, 1987, 1991), Swift and Koltermann (1988), Rudels (1986), Rudels and Quadfasel (1991), Jones et al. (1995), and Schlichtholz and Houssais (1999) have revealed a major contribution of Norwegian Sea Deep Water (NSDW) to the deeper water masses in the eastern Fram Strait, which is considered to form by mixing of waters from the polar oceans in the Greenland Sea (Rudels and Quadfasel, 1991).

Studies of the past behaviour of the two-way exchange system in the Fram Strait provide insight on the variations of the interaction between the Arctic Ocean and the Nordic Seas. Compared to glacial periods, climate variations during the Holocene period (since ca 11.7 cal ka BP) were generally of smaller amplitude but nevertheless significant. The eastern Fram Strait has been particularly affected by variations of AW inflow and sea-ice extent during the Holocene. Enhanced inflow of warm and saline AW coinciding with maximum insolation (e.g., Laskar et al., 2004) resulted in relatively high sea surface temperatures west of Svalbard during the Early and Mid-Holocene (e.g., Sarnthein et al., 2003; Hald et al., 2004, 2007). A southeast advance of cold Arctic waters and the summer sea-ice margin, as well as a concurrent weakening of the AW inflow after ca 5 cal ka BP was associated with the Neoglacial cooling trend of the Late Holocene (Werner et al., 2013). Here, we use a radiogenic isotope approach, supported by new data from microfossil assemblages and their isotopic composition, to elucidate Holocene variations of water mass exchange between the Nordic Seas and the Arctic Ocean, and to identify the possible influence of the discharge of sea-ice sediments on the bottom water chemistry.

2. Detailed hydrographic setting

The subsurface AW advection through eastern Fram Strait is the main heat source of the Arctic Ocean (Schauer et al., 2004). The AW inflow is characterized by relatively warm and saline water masses (summer temperatures $\leq 6\,^{\circ}C$, $S \leq 35.2$; Spielhagen et al., 2011) and is topographically constrained to the eastern Fram Strait. It reaches a thickness of up to 700 m at the Western Svalbard margin (Schlichtholz and Goszczko, 2006) and is advected into the Arctic Ocean via the WSC, which is the northward propagation of the Norwegian Atlantic Current (NAC). Close to the study area (Fig. 1), AW submerges beneath an about 100 m thick cold and fresh upper mixed layer of Arctic origin and continues as a subsurface current into the Arctic Ocean (Johannessen, 1986). On its way north, the top of the AW layer further encounters and melts Arctic sea ice and contributes to the production of the low-salinity mixed layer at the surface (Rudels et al., 2005). As a consequence, a large part of the eastern Fram Strait remains ice-free even in winter (e.g., Vinje, 2001).

Between intermediate and abyssal depths, the WSC transports AIW and NSDW, respectively. NSDW dominates the deepwater inflow through eastern Fram Strait (e.g., Aagaard et al., 1985; Swift and Koltermann, 1988; Jones et al., 1995; Fig. 2) and has most likely been the water mass prevailing at the site of our study. It is characterized by temperatures between −1.1 and 0 °C and a salinity range of 34.90–34.92 (Schlichtholz and Houssais, 1999; Fig. 2). The NSDW at our site forms by mixing of some older NSDW arriving from the Nordic Seas with Arctic Ocean Deep Waters from different sources, such as Upper Polar Deep Water, Eurasian Basin Deep Water and Canadian Basin Deep Water (Schlichtholz and Houssais, 1999). For a detailed description of the individual water masses we refer to the studies by Schlichtholz and Houssais (1999) and Rudels et al. (2000, 2002, 2005). Since deepwater inflow from the Nordic Seas has been detected in the western Fram Strait at ca 78°50′N (Rudels et al., 2005) and at the northern slope of Yermak Plateau (Jones et al., 1995) where it most likely merges with Eurasian Basin Deep Water (Rudels et al., 2005), it obviously passes our study site at 78°55′N on its way into the Arctic Ocean.

In the western part of the Fram Strait cold and fresh polar surface waters and sea ice are transported southward with the East Greenland Current (EGC, Fig. 1). Waters of the EGC are formed by mixing of southward-flowing less dense Polar Water ($T < 0\,^{\circ}C$, $S < 34.5$; e.g., Falck et al., 2005) with deeper waters from the Arctic Ocean (Budéus and Ronski, 2009). While a considerable fraction of surface and subsurface waters of the EGC down to 200 m depth has been identified to be of Pacific origin (Jones et al., 2003), cooled Atlantic Water either returning within the Fram Strait as the Recirculation Atlantic Current (RAC; Rudels et al., 2005) or flowing out from the Arctic basin (Arctic Atlantic Water, AAW) is entrained into the southward directed EGC in the western Fram Strait at intermediate depth (e.g., Marnela et al., 2008).

3. Radiogenic isotopes

Studies of radiogenic Nd and Pb isotope compositions of past seawater have achieved increasing attention in paleoceanographic

Fig. 1. **a**) Map of the Arctic Ocean (IBCAO; Jakobsson et al., 2012) with surface, intermediate, and deepwater currents of the Nordic Seas and the Arctic Ocean (JMFZ = Jan Mayen Fracture Zone, MJR = Morris Jesup Rise, Sv. = Svalbard). Dark blue dashed arrows in the Arctic Ocean basins show schematic circulation of the Upper Polar Deep Water down to depths of about 1700 m (Jones, 2001). Dark blue dashed arrows in the Nordic Seas and the Fram Strait indicate large-scale intermediate and deep circulation modified from Lacan and Jeandel (2004b). Light blue arrows reflect cold and fresh surface waters of Arctic origin. Red arrows indicate warm and saline Atlantic Water inflow through Fram Strait and the Barents Sea. The yellow star marks the investigated core site MSM5/5-712 which is influenced by Atlantic Water at subsurface and admixture of Arctic Intermediate and Norwegian Sea Deep Water at intermediate and abyssal depths, respectively. Black squares refer to present-day seawater ε_{Nd} values from literature (Piepgras and Jacobsen, 1988; Lacan and Jeandel, 2004a,b; Dahlqvist et al., 2007; Andersson et al., 2008; Amakawa et al., 2009; Porcelli et al., 2009; Zimmermann et al., 2009). White ovals mark average ε_{Nd} values of sediment leachates in the Kara Sea (Chen et al., 2012; Haley and Polyak, 2013), white triangle indicates average ε_{Nd} value of sea-ice sediment (detritus) after Tütken et al. (2002). White hexagons show ε_{Nd} value of rock material for Greenland (Lacan and Jeandel, 2004a), for the western Norwegian Caledonian margin (Lacan and Jeandel, 2004b and references therein), for West Siberia (Polar Ural: Edwards and Wasserburg, 1985; Putorana Basalts: Sharma et al., 1992). **Inset**: The main sea-ice drift streams Transpolar Drift (TPD) and Beaufort Gyre (BG) of the Arctic Ocean. **b**) Nd isotope composition of ferromanganese coatings from core top samples in the eastern Fram Strait (yellow ovals, see also Table 1). For comparison, selected seawater ε_{Nd} values from the Fram Strait are shown (blue rectangles: this study, Table 2; black rectangles compiled from Lacan and Jeandel, 2004a,b; Andersson et al., 2008). Arrows mark prevailing surface/subsurface current system of warm and saline Atlantic Water inflow (red) and cold and fresh Arctic outflow waters (blue). Also shown is the approximate summer sea-ice margin (white dashed line). White hexagons indicate ε_{Nd} values of Svalbard rock material compiled from the literature (Peucat et al., 1989; Johansson and Gee, 1999; Johansson et al., 2002; Tütken et al., 2002 and references therein; Andersson et al., 2008 and references therein). Green line marks approximate cross section of eastern Fram Strait at 78.5°N shown in Fig. 2.

Please cite this article in press as: Werner, K., et al., Neoglacial change in deep water exchange and increase of sea-ice transport through eastern Fram Strait: evidence from radiogenic isotopes, Quaternary Science Reviews (2013), http://dx.doi.org/10.1016/j.quascirev.2013.06.015

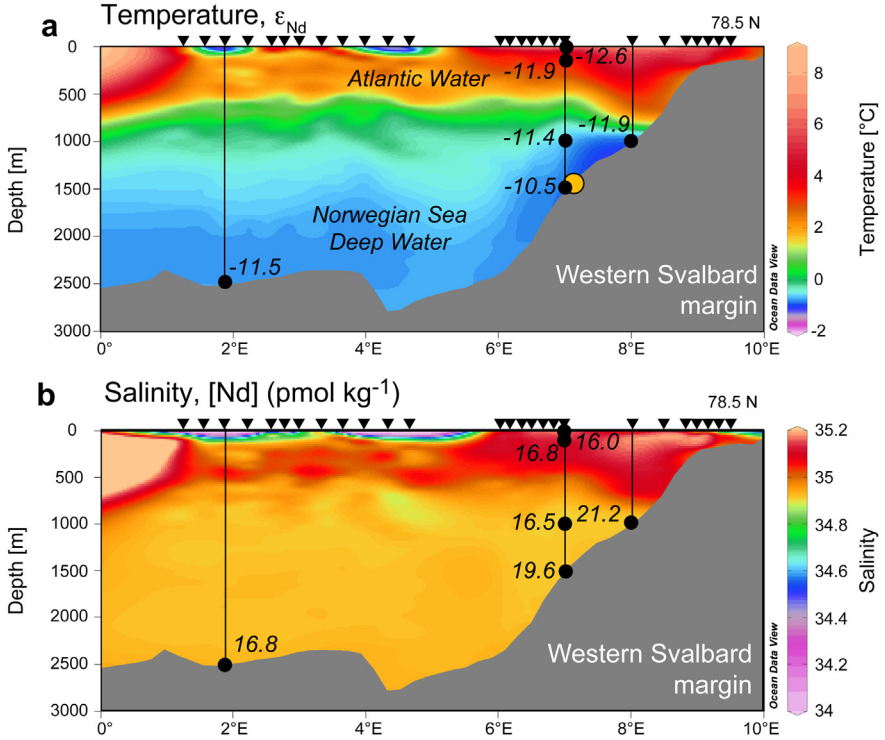

Fig. 2. Cross section of eastern Fram Strait (Ocean Data View; Schlitzer, 2007) at 78.5°N with locations of seawater samples investigated for **a**) Nd isotope composition ε_{Nd} and **b**) Nd concentrations [Nd] and respective temperatures and salinities in the water column obtained during R/V Polarstern cruise leg ARK-XXVI/1 (Beszczynska-Möller and Wisotzki, 2012; black triangles indicate mooring stations). Yellow dot marks approximate position of sediment core 712 on the West Spitsbergen continental margin.

and paleoclimate reconstructions over the past ca 15 years (e.g., van de Flierdt and Frank, 2010). Of particular advantage is the independence of radiogenic isotopes from stable isotope fractionation induced by biological activity or physical processes (e.g., van de Flierdt et al., 2006; Gutjahr et al., 2007). The average oceanic residence time of Nd is between 400 and 2000 years (Tachikawa et al., 1999; Frank, 2002; Arsouze et al., 2009; Rempfer et al., 2011), which is similar to the global mixing time of the oceans (about 1500 years; Broecker, 1982). Remote from continental inputs, water masses only change their Nd isotope signatures originating from their source areas by mixing with other water masses and thus serve as quasi-conservative tracers of ocean circulation (e.g., Piepgras and Wasserburg, 1980; Frank, 2002). Variations of the $^{143}Nd/^{144}Nd$ ratio are expressed as $\varepsilon_{Nd} = [(^{143}Nd/^{144}Nd_{Sample})/(^{143}Nd/^{144}Nd)_{CHUR} - 1]$ *10.000 [CHUR (*Chondritic Uniform Reservoir*) is the present-day average earth value of 0.512638; Jacobsen and Wasserburg, 1980].

Dissolved radiogenic isotope signatures in seawater originate from weathering processes of the continental crust. They are delivered in dissolved or detrital form via riverine and eolian inputs to the ocean where they subsequently partly dissolve or exchange with seawater (e.g., Frank, 2002). In addition, sediment transport via sea ice/icebergs and subsequent release of ice rafted debris (IRD) upon melting is another important sediment source in the Arctic Ocean, which also exerts its influence on the dissolved radiogenic isotope composition of seawater. Margin/seawater interactions (boundary exchange) must be considered as a further source for radiogenic isotope signatures of seawater, in particular in the Nordic Seas where basaltic formations highly susceptible to dissolution and to exchange with seawater can exert strong influence (e.g., Lacan and Jeandel, 2004b, 2005).

High particle reactivity of Pb accounts for its shorter residence time of about 50 years in the ocean (e.g., Frank, 2002, and references therein; Haley et al., 2008b) and thus makes it a useful tracer for local changes of weathering input to the ocean and short distance water mass transport and mixing (cf. Stumpf et al., 2010). In surface waters, the residence time of Pb is even shorter (<5 years) (Hamelin et al., 1990). In today's oceans all natural Pb isotope compositions in seawater are overprinted by anthropogenic Pb (e.g., Schaule and Patterson, 1981). In the Arctic Ocean where a considerable portion of sediment material is released by sea ice, anthropogenic Pb contamination is pronouncedly reflected in the surface sediments (Gobeil et al., 2001).

Under oxic conditions, radiogenic isotopic compositions of bottom waters are incorporated and preserved in authigenic ferromanganese oxyhydroxide coatings of bottom sediments and can be directly extracted from bulk sediments applying reductive leaching procedures (Rutberg et al., 2000; Bayon et al., 2002; Gutjahr et al., 2007; Stumpf et al., 2010). This approach has been previously applied successfully to sediments in the Arctic Ocean and in the North Atlantic for both pre-Quaternary and Quaternary studies (e.g., Haley et al., 2008a,b; Crocket et al., 2011; Chen et al., 2012; Haley and Polyak, 2013; Jang et al., 2013). Studies of the Nd isotope composition of the leachable seawater-derived fraction of central Arctic Ocean sediments on the Lomonosov Ridge at 1100 m water depth revealed that AW has dominated the interglacial deep waters at this site whereas brine formation on the Siberian shelf, in particular in the Kara Sea region, together with a diminished AW inflow caused much more radiogenic Nd isotope compositions during glacial times in the central Arctic Ocean (Haley et al., 2008a; Jang et al., 2013). Sediment leachates of core top samples on the Kara Sea shelf recently confirmed this origin of radiogenic Nd isotope compositions between −6.1 and −3.4 (Fig. 1; Chen et al., 2012; Haley and Polyak, 2013) which were most likely caused by riverine input and subsequent exchange with radiogenic weathering products of the Putorana basalts ($\varepsilon_{Nd} \geq 0$; Sharma et al., 1992) in the Siberian hinterland (e.g., Haley et al., 2008a; Chen et al., 2012; Haley and Polyak, 2013).

Please cite this article in press as: Werner, K., et al., Neoglacial change in deep water exchange and increase of sea-ice transport through eastern Fram Strait: evidence from radiogenic isotopes, Quaternary Science Reviews (2013), http://dx.doi.org/10.1016/j.quascirev.2013.06.015

The radiogenic isotope compositions (Nd, Pb, Sr) of the detrital fraction of the sediments determined on the same samples (Haley et al., 2008b), as well as for other sediment cores near Svalbard (Eisenhauer et al., 1999; Tütken et al., 2002) were used to reconstruct the provenance of the detrital sediments over the past 15 million years and revealed a significant contribution of sea-ice rafted material from the Siberian shelves to central Arctic and the Fram Strait bottom sediments.

The goal of this study is to reconstruct changes in Holocene bottom and surface water mixing and to detect the influence of weathering inputs from nearby landmasses by investigating the radiogenic Nd and Pb isotopic signatures of bottom waters and of sediment supply on the Western Svalbard continental margin over the past ca 8.5 ka. We apply seawater-derived radiogenic isotope compositions extracted from authigenic ferromanganese oxyhydroxide coatings of bottom sediments to elucidate Holocene variations of water mass exchange between the Nordic Seas and the Arctic Ocean. These data also allow to reconstruct the influence of the discharge of sea-ice sediments to seawater, which has influenced sediment composition in the eastern Fram Strait, an area which is today located near the fluctuating summer sea-ice margin. Radiogenic isotope data from leachates and detrital material are combined with high-resolution multiproxy data reflecting Holocene surface/subsurface and bottom water conditions on the West Spitsbergen continental margin (see also Spielhagen et al., 2011; Werner et al., 2011, 2013; Müller et al., 2012). These proxies include planktic foraminiferal assemblages, planktic and benthic stable isotope records, as well as indicators for past sea-ice variability. In order to obtain a calibration of the Nd isotope compositions extracted from the sediments to modern bottom water mass signatures in the area, a set of core top and water samples from different water depths in the eastern Fram Strait has been analysed.

4. Material and methods

4.1. Sampling and sample preparation

Samples for investigation of Nd and Pb isotope compositions were obtained from two sediment cores (kastenlot and box core) recovered from station MSM5/5-712 at the western Svalbard continental margin (78°54.94′N, 6°46.04′E, 1490.5 m water depth, Fig. 1) during cruise leg MSM5/5 of the RV “Maria S. Merian” in summer 2007. Core top samples were obtained on the same cruise (for locations and water depths see Table 1). Detailed stratigraphy and proxy datasets of box core MSM5/5-712-1 covering the past ca 2000 years were reported in Spielhagen et al. (2011) and Werner et al. (2011). Chronology and multiproxy records of the uppermost 210 cm of kastenlot core MSM5/5-712-2 are presented in Müller et al. (2012) and Werner et al. (2013). Given that the downcore data presented here are a combination of records from both box core 712-1 and kastenlot core 712-2 we will refer to the entire downcore record as 712 if not marked otherwise.

Extraction of seawater Nd, Pb, and Sr isotope signals from ferromanganese coatings of bulk sediments was carried out following a slightly modified version of the methods of Gutjahr et al. (2007) and Stumpf et al. (2010). Samples were processed in acid-cleaned polypropylene 50 ml centrifuge tubes. About 2 g of freeze-dried and coarsely ground bulk sediment material were rinsed twice with 20 ml of deionised water (Milli-Q system, MQ water). To remove carbonate, samples were treated with a 44%-acetic acid/1M-Na acetate buffer. For the leaching process to dissolve the ferromanganese oxyhydroxide coatings, about 20 ml of the leaching solution (0.05 M-hydroxylamine hydrochloride/15%-acetic acid solution buffered to pH 3.6 with NaOH) was added to the samples and left to react in an ultrasonic bath for 1 h and in a

Table 1
Locations and Nd, Pb, and Sr isotope data from leachable and detrital fractions of core top samples from the eastern Fram Strait.

Sample name	Water depth (m)	Latitude (N)	Longitude (E)	Leachates					Detrital fraction				
				ε_{Nd} ± 0.28	$^{206}Pb/^{204}Pb$ ± 0.0075	$^{207}Pb/^{204}Pb$ ± 0.0101	$^{208}Pb/^{204}Pb$ ± 0.0326	$^{86}Sr/^{87}Sr$ ± 0.00002	ε_{Nd} ± 0.18	$^{206}Pb/^{204}Pb$ ± 0.0048	$^{207}Pb/^{204}Pb$ ± 0.0050	$^{208}Pb/^{204}Pb$ ± 0.0134	$^{86}Sr/^{87}Sr$ ± 0.00001
712-1	1490.5	78°54.94′	6°46.04′	−9.1	18.441	15.610	38.333	0.71109	−11.4	18.647	15.613	38.567	0.73142
715-3	1480.5	79°11.98′	6°15.24′	−10.2	18.472	15.615	38.357	0.71020	−11.0	18.658	15.620	38.568	–
716-2	1253.9	79°14.11′	7°13.26	–	18.400	15.608	38.304	0.71144	–	–	–	–	–
718-1	1334.9	79°42.92′	5°56.52′	–	18.481	15.609	38.353	0.71174	–	–	–	–	–
723-1	1350.7	79°09.66′	5°20.27′	−9.7	18.457	15.616	38.341	0.71029	−10.9	18.630	15.628	38.555	–
725-2	1960	80°57.00′	11°19.37′	−9.2	18.573	15.618	38.493	0.71001	−9.1	18.701	15.624	38.661	0.72549

shaker for 1 h. After centrifugation, the supernatant containing the dissolved seawater fraction of the coatings was pipetted off into Teflon vials for further chemical treatment. In addition, about 30 mg of MQ-washed residual bulk sediment material were treated with aqua regia, concentrated HNO_3 and HF to completely dissolve the detrital silicate fraction and destroy organic matter.

A set of water samples from different depths in the eastern Fram Strait was obtained during cruise leg ARK-XXVI/1 of RV "Polarstern" in summer 2011. Locations and water depths are reported in Table 2. Samples were collected with a rosette equipped with 24 Niskin-type sample bottles and a conductivity-temperature-depth (CTD) unit. The seawater was transferred into 20 L acid-cleaned polyethylene containers. In the home laboratory seawater samples were filtered (<45 μm) and acidified to pH ~2 with concentrated HCl. Between 10 and 20 L of the filtered water samples were used for analysing the dissolved Nd isotope ratios. About 0.5 ml $FeCl_2$ solution/20 L water was added to coprecipitate Nd. After equilibration for more than 24 h, ammonia solution (25%, suprapure) was added to reach a pH ~8 in order to coprecipitate dissolved trace metals with FeOOH. The supernatant was discarded and the FeOOH precipitates were thoroughly washed and centrifuged. The Fe-precipitate was then dissolved in HCl and aqua regia to destroy organic components. Fe was removed from the samples by using liquid–liquid extraction with cleaned di-ethyl ether. The Nd concentrations were determined using a $^{150}Nd/^{149}Sm$ double spike solution as described in Rickli et al. (2009).

4.2. Separation and purification of Pb, Nd, and Sr

We followed standard procedures for ion chromatographic separation and purification of the elements for the water and sediment samples (for Nd: Cohen et al., 1988; Barrat et al., 1996; Le Fèvre and Pin, 2005; for Pb: Galer and O'Nions, 1989; Lugmair and Galer, 1992; and for Sr: Horwitz et al., 1992; Bayon et al., 2002). Separation of Pb was carried out on cation exchange columns (50 μl AG1-X8 resin, mesh size 100–200 μm). Alkaline elements were separated from rare earth elements (REEs) on cation exchange columns (0.8 ml AG50W-X12 resin, mesh size 200–400 μm). Separation of Nd from the other REEs was carried out on columns with 2 ml Ln Spec resin (mesh size 50–100 μm). Purification of Sr was achieved on columns filled with 50 μl Sr Spec resin (mesh size 50–100 μm).

4.3. Isotope measurements

Nd, Pb, and Sr isotope analyses were carried out on a Nu Plasma MC-ICPMS at GEOMAR, Kiel. All Nd isotope ratios ($^{143}Nd/^{144}Nd$) presented were corrected for mass bias following an exponential law using ($^{146}Nd/^{144}Nd = 0.7219$) and normalized to the accepted value of the JNdi-1 standard of 0.512115 (Tanaka et al., 2000). Repeated measurements of the JNdi-1 standard ($n = 69$) gave long-term external reproducibility between 0.17 and 0.29 ε_{Nd} units (2σ).

A standard bracketing method following Albarède et al. (2004) was applied to determine Pb isotope ratios. All presented Pb isotope values were normalized to the accepted values for the NBS981 standard (Abouchami et al., 1999). The 2σ reproducibility for NBS981 was 0.0048–0.0075 for $^{206}Pb/^{204}Pb$, 0.0050–0.0101 for $^{207}Pb/^{204}Pb$, and 0.0134–0.0326 for $^{208}Pb/^{204}Pb$ (for details see Tables 1 and 3).

$^{87}Sr/^{86}Sr$ ratios were corrected for isobaric interference (^{86}Kr, ^{87}Rb) and mass bias (using $^{86}Sr/^{88}Sr = 0.1194$; Steiger and Jäger, 1977). All Sr isotope data were normalized to the accepted value of standard NBS987 ($^{87}Sr/^{86}Sr = 0.710245$). The 2σ external reproducibility during measurements was between 0.00001 and 0.00002 (for details see Tables 1 and 3).

5. Results

5.1. Present-day seawater ε_{Nd} signatures in the eastern Fram Strait

The measured seawater samples from one water profile (25–1400 m) and from two bottom water locations in the eastern Fram Strait (Table 2) are in good agreement with previous studies of the modern seawater ε_{Nd} distribution in this area. Atlantic Water entering the eastern Fram Strait from the south at subsurface to intermediate water depth is less radiogenic (ε_{Nd} ~−11.9; Table 2, Fig. 2) than deeper flowing NSDW (ε_{Nd} ~−10.5, Fig. 1; see also Lacan and Jeandel, 2004b). The latter has acquired a more radiogenic ε_{Nd} signature between −10.1 (1500 m water depth) and −10.5 (3400 m water depth) through margin/seawater interactions when flowing along the highly radiogenic Norwegian Basin basaltic margins (i.e., the islands of Jan Mayen, Iceland, and Faroe; Lacan and Jeandel, 2004b). In the Nansen and Makarov basins of the Arctic Ocean, these Nordic Seas-derived waters were characterized by similar ε_{Nd} signatures of −10.9 and −10.5, respectively (Porcelli et al., 2009) in agreement with the AW pathway at intermediate depths of the Arctic Ocean (Rudels et al., 1994). The ε_{Nd} value near 2500 m water depth at 2° E in the eastern Fram Strait is somewhat less radiogenic (−11.5) and may not be influenced by the above boundary exchange processes to the same extent. Similarly, within polar surface waters (at 25 m water depth) we measured an ε_{Nd} value of ~−12.6, which is in good agreement with other profiles near Svalbard (Andersson et al., 2008) where the outcropping rocks have unradiogenic ε_{Nd} values of up to −14 (Tütken et al., 2002).

More radiogenic ε_{Nd} values in the northwestern Fram Strait characterize the cold and fresh Arctic outflow waters of both surface and deeper waters down to 1300 m water depth (~−9.5; Andersson et al., 2008; Fig. 1). Relatively radiogenic Pacific waters enter through Bering Strait (ε_{Nd} ~−5; Piepgras and Jacobsen, 1988) and through vertical exchange processes contribute to the

Table 2
Locations and Nd isotope and concentration data of seawater samples from the eastern Fram Strait obtained during Polarstern cruise leg ARK-XXVI/1. Also shown are CTD-derived salinity and temperature of the respective water sample (Beszczynska-Möller and Wisotzki, 2012).

Station name	Latitude (N)	Longitude	Water depth (m)	ε_{Nd}	C_{Nd} (pmol kg^{-1})	Salinity	Temperature (°C)
PS78/127	78°49.82′	8°10.00′E	987	−11.9[a]	21.2	34.91	−0.8
PS78/025	78°50.05′	7°00.20′E	25	−12.6[b]	16.0	35.17	6.3
			150	−11.9[b]	16.8	35.10	3.2
			1000	−11.4[a]	16.5	34.91	−0.7
			1416	−10.5[c]	19.6	34.91	−0.9
PS78/039	78°49.65′	1°52.79′E	2496	−11.5[a]	16.8	34.92	−0.8

[a] $2\sigma \pm 0.29$.
[b] $2\sigma \pm 0.27$.
[c] $2\sigma \pm 0.17$.

Please cite this article in press as: Werner, K., et al., Neoglacial change in deep water exchange and increase of sea-ice transport through eastern Fram Strait: evidence from radiogenic isotopes, Quaternary Science Reviews (2013), http://dx.doi.org/10.1016/j.quascirev.2013.06.015

Table 3
Core depths, calibrated ages and Nd, Pb, and Sr isotope data of the leachable and detrital fractions in sediment core 712. Ages of box core 712-1 are also given in year AD.

Sediment core	Depth interval (cm)	Cal age, yr BP/ age, yr AD	Leachates					Detrital fraction				
			ε_{Nd} ± 0.28	$^{206}Pb/^{204}Pb$ ± 0.0075	$^{207}Pb/^{204}Pb$ ± 0.0101	$^{208}Pb/^{204}Pb$ ± 0.0326	Sr ± 0.00002	ε_{Nd} ± 0.18	$^{206}Pb/^{204}Pb$ ± 0.0048	$^{207}Pb/^{204}Pb$ ± 0.0050	$^{208}Pb/^{204}Pb$ ± 0.0134	Sr ± 0.00001
712-1	Core top	>1960 AD (−57/2007)[a]	−9.1	18.441	15.610	38.333	0.71109	−11.4	18.647	15.613	38.567	0.73142
	0.0–0.5	−48/1998	–	18.461	15.619	38.350	0.71024	–	–	–	–	–
	2.5–3.0	40/1910	−10.2	18.444	15.617	38.335	0.71016	−11.1	18.611	15.626	38.544	0.72043
	5.0–5.5	128/1822	–	18.573	15.628	38.513	0.71010	–	–	–	–	–
	10.0–10.5	305/1645	−9.2	18.787	15.637	38.726	0.71001	−11.5	18.967	15.633	39.037	0.72087
	15.0–15.5	492/1458	−9.0	18.899	15.630	38.793	0.71023	−11.2	19.004	15.639	38.991	0.72100
	20.0–20.5	769/1181	−8.8	18.952	15.641	38.867	0.71000	−10.9	19.059	15.641	39.017	0.72030
	25.0–25.5	1027/923	−8.9	19.009	15.642	38.901	0.71006	−11.1	19.021	15.633	38.978	0.72142
	30.0–30.5	1278/672	−8.9	19.013	15.640	38.908	0.71001	−11.1	19.014	15.636	38.983	0.72094
	35.5–36.0	1559/391	–	19.039	15.649	38.950	0.71011	–	–	–	–	–
	40.0–40.5	1789/161	−9.0	19.064	15.664	39.001	0.71027	−11.5	19.034	15.631	38.916	0.72200
712-2	52.0–53.0	2810	−10.0	19.149	15.663	39.041	0.71014	−12.3	19.061	15.632	38.953	0.72258
	62.0–63.0	3352	−9.5	19.100	15.654	38.994	0.71015	−11.7	19.015	15.633	38.919	0.72121
	76.0–77.0	4167	−10.1	19.127	15.654	39.004	0.71017	−12.1	19.064	15.637	38.977	0.72303
	95.0–96.0	5252	−9.7	19.150	15.657	39.013	0.71006	−12.0	19.007	15.635	38.879	0.72222
	110.5–111.5	5849	−10.4	19.165	15.662	39.024	0.71002	−12.2	19.031	15.632	38.894	0.72319
	119.5–120.5	6195	−10.5	19.165	15.663	39.024	0.71017	−12.1	19.039	15.639	38.968	0.72255
	185.5–186.5	8141	−10.1	19.212	15.670	39.071	0.70996	−12.4	19.082	15.641	38.938	0.72385
	200.5–201.5	8534	−10.6	19.135	15.652	38.975	0.71014	−12.0	19.052	15.634	38.950	0.72372

[a] Bomb radiocarbon.

relatively radiogenic seawater ε_{Nd} values of −9 found in deeper waters (2500 m) of the Canada Basin (Porcelli et al., 2009; Fig. 1). Since Pacific contributions to subsurface waters of up to 200 m depths can be clearly traced crossing the Arctic Ocean and entering the Fram Strait in its northwestern part (e.g., Jones et al., 2003; Björk et al., 2010), radiogenic Nd isotope signatures of seawater found in the western Fram Strait most likely have their origin in mixing with subsurface waters from the Canadian Basin (Andersson et al., 2008; Porcelli et al., 2009).

Riverine input from the Arctic shelves, and in particular from the Siberian margin, is another significant component of Arctic waters. The discharge of the rivers Lena, Ob and Yenisey accounts for half of the entire river runoff into the Arctic Ocean (Aagaard and Carmack, 1989, and references therein). Through water–shelf interactions during winter, such as sea-ice formation and associated sinking of dense brine waters (Bauch et al., 1995), river waters can significantly alter the seawater ε_{Nd} signatures on the shelves (Porcelli et al., 2009). While the eastern Laptev Sea shelf waters are relatively unradiogenic ($\varepsilon_{Nd} \sim -14$), more radiogenic riverine inputs of the rivers Yenisey and Ob ($\varepsilon_{Nd} \sim -5$ and −6, respectively) strongly contribute to the radiogenic Nd isotope compositions of the Kara Sea shelf waters (Porcelli et al., 2009; Zimmermann et al., 2009, Fig. 1).

Measured Nd concentrations in the seawater samples range between 16.0 and 21.2 pmol/kg. Nd concentrations within the Atlantic Water layer exhibit C_{Nd} values ≥16.0 pmol/kg. Unlike data of Andersson et al. (2008) and Porcelli et al. (2009) our snapshot of seawater samples from June 2011 does not show enrichment of Nd in surface waters due to addition of Nd from Svalbard shelf sediments (Andersson et al., 2008) but indicate higher concentrations near the sediment water interface (1000–1400 m water depths) which might point to release processes effective at the Svalbard margin.

5.2. Radiogenic isotope compositions of the sediments

Sediment coatings of core top samples show radiogenic ε_{Nd} values ranging from −9.1 to −9.7 except for station 715-3 which displays a less radiogenic ε_{Nd} value of −10.2 (Table 1; Figs. 1b and 3). Since the AMS radiocarbon dating of the core top sample at station 712-1 (1490 m water depth) based on shells of planktic foraminifera revealed a modern age containing bomb radiocarbon (Spielhagen et al., 2011) we are confident that the surface ε_{Nd} value of −9.1 represents the present-day value for station 712-1. Likewise, we infer similar present-day ε_{Nd} values for the West Spitsbergen continental margin as corroborated by core top measurements presented in this study (Table 1, Fig. 3). The unradiogenic ε_{Nd} value (−10.2) at station 715-3 is consistent with present-day seawater ε_{Nd} values of North Atlantic Drift waters obtained in the eastern Fram Strait (Figs. 1 and 2, Table 2) and further south in the Nordic Seas, as well as in the western Fram Strait area under the influence of the East Greenland Current (Lacan and Jeandel, 2004a; Fig. 1). Because all other core top stations located close to the site of 715-3 reveal values of −9.1 to −9.7, we assume that station 715-3, which was not ^{14}C-dated, represents an age older than 2000 years leading to an ε_{Nd} signature similar to those found in the downcore record of 712 for the interval between 8.5 and 2.8 cal ka BP (ε_{Nd} −10.6 to −10.0; see below). Such high surface sediment ages, resulting from low sedimentation rates and bioturbation, are not uncommon at places in the Fram Strait and the Arctic Ocean (Nørgaard-Pedersen et al., 2003; Spielhagen, unpubl. data).

Except for the northernmost core top station 725-3 the detrital fraction of the surface samples reveals less radiogenic ε_{Nd} signatures (between −11.4 and −10.9) than the leached data. Detrital

Please cite this article in press as: Werner, K., et al., Neoglacial change in deep water exchange and increase of sea-ice transport through eastern Fram Strait: evidence from radiogenic isotopes, Quaternary Science Reviews (2013), http://dx.doi.org/10.1016/j.quascirev.2013.06.015

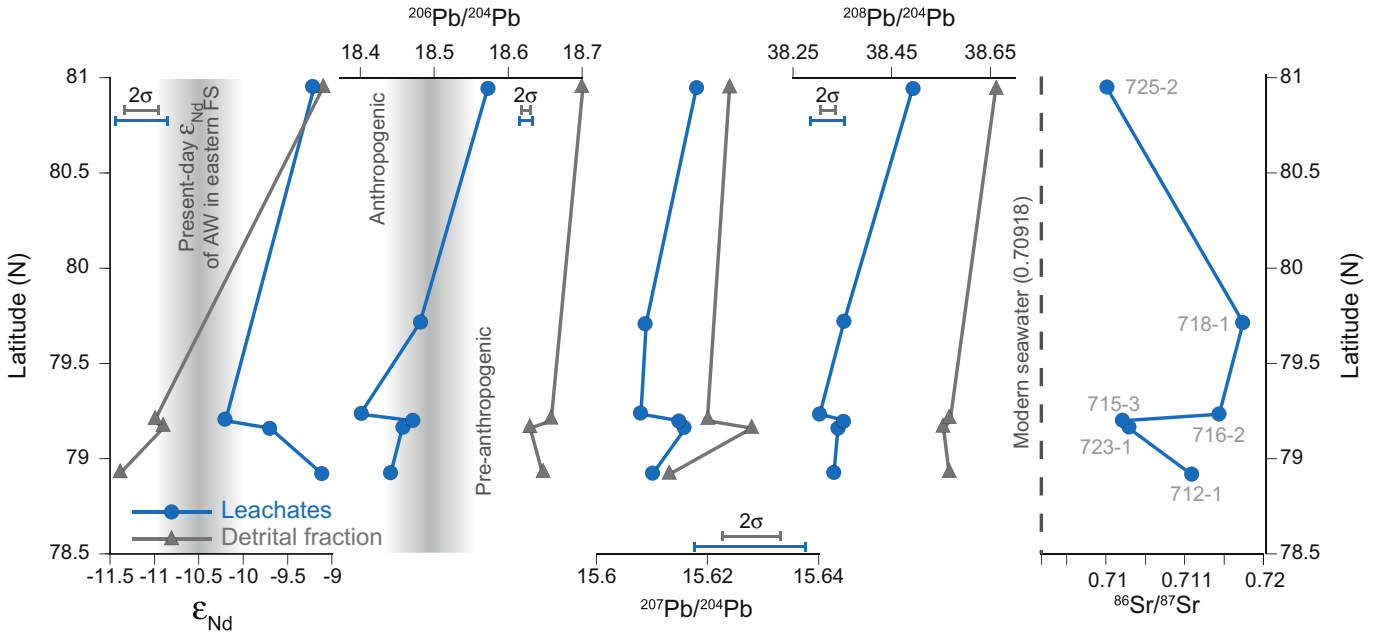

Fig. 3. Nd, Pb, and Sr record of leachate (blue dots) and detrital (grey triangles) material of core top samples vs. latitude. Anthropogenic and pre-anthropogenic $^{206}Pb/^{204}Pb$ taken from Gobeil et al. (2001). Numbers and approximate position of core top stations are indicated in $^{86}Sr/^{87}Sr$ figure on the right. Modern $^{86}Sr/^{87}Sr$ seawater value after Henderson et al. (1994). The range of the 2σ error for $^{86}Sr/^{87}Sr$ is smaller than the symbol. (For interpretation of the references to colour in this figure legend, the reader is referred to the web version of this article.)

material from station 725-3 displays a more radiogenic ε_{Nd} value of −9.1, similar to its leachate value (−9.2), (Table 1; Fig. 3).

$^{206}Pb/^{204}Pb$ data from the core top sediment leachates show highly unradiogenic values near ~18.4 (Table 1, Fig. 3). These $^{206}Pb/^{204}Pb$ compositions of the eastern Fram Strait stations are consistent with the range of anthropogenic $^{206}Pb/^{204}Pb$ values reported for Western European sources (Véron and Church, 1997) and for the Greenland Sea and Eurasian basin (17.75–18.38; Gobeil et al., 2001; Fig. 3) which is also reflected in other leachate Pb isotope ratios shown in Fig. 3. Site 725-2 north of Svalbard reveals slightly more radiogenic values near 18.6 which might indicate a stronger dilution of anthropogenic Pb with natural Pb within the bioturbated mixed-layer (Hamelin et al., 1990) and an associated older age of this core top sample. The detrital residues of the core top samples show generally more radiogenic Pb isotope values than the leachates but still contain a significant anthropogenic signature.

During the past ca 8500 years, seawater-derived ε_{Nd} signatures varied between −10.6 and −8.8 (Table 3, Fig. 4). A general trend to

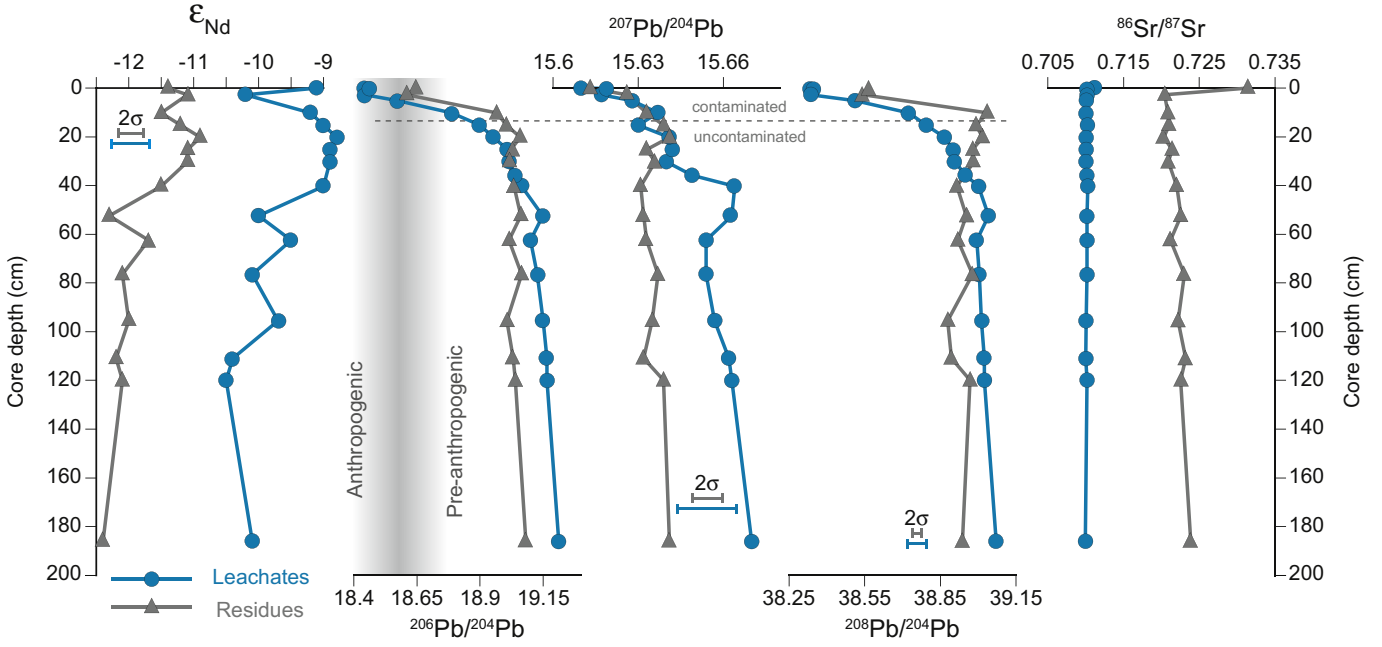

Fig. 4. Nd, Pb, and Sr record of leachate (blue dots) and detrital (grey triangles) material in the uppermost 200 cm of sediment core MSM5/5-712. Ranges of the 2σ errors for $^{86}Sr/^{87}Sr$ and $^{206}Pb/^{204}Pb$ are smaller than the symbols. (For interpretation of the references to colour in this figure legend, the reader is referred to the web version of this article.)

Please cite this article in press as: Werner, K., et al., Neoglacial change in deep water exchange and increase of sea-ice transport through eastern Fram Strait: evidence from radiogenic isotopes, Quaternary Science Reviews (2013), http://dx.doi.org/10.1016/j.quascirev.2013.06.015

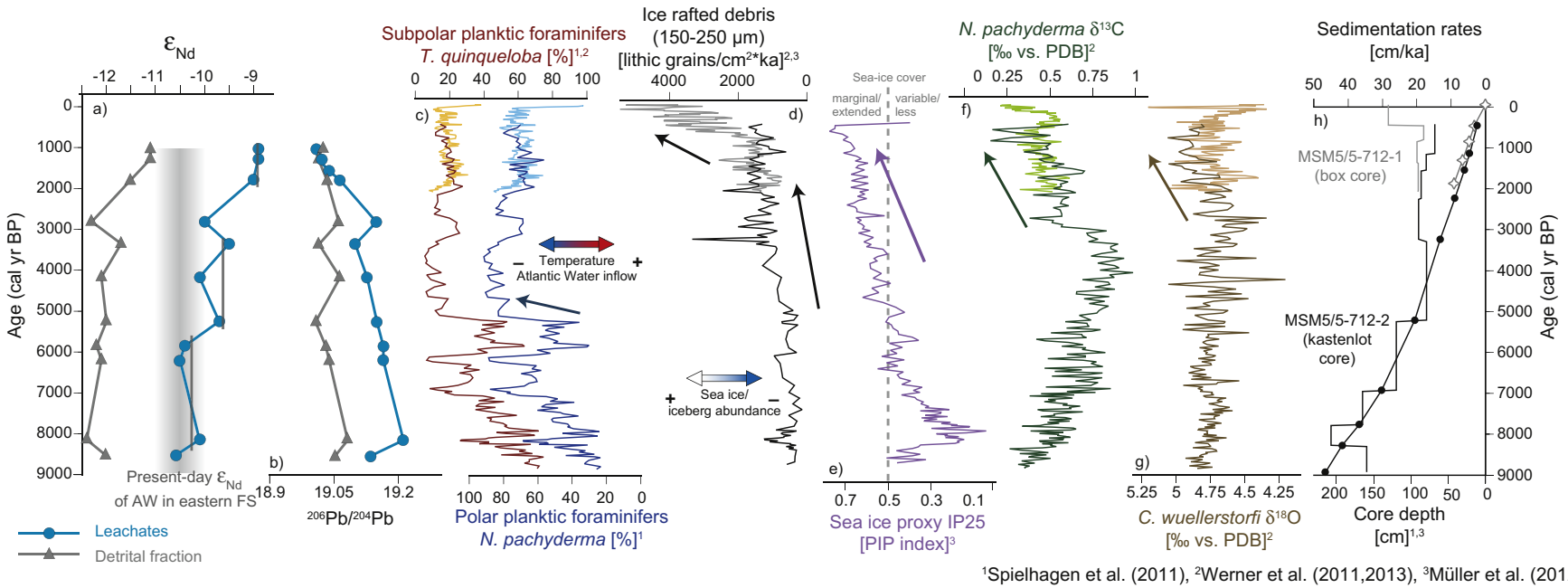

[1]Spielhagen et al. (2011), [2]Werner et al. (2011,2013), [3]Müller et al. (2012)

Fig. 5. Downcore (**a**) Nd and (**b**) Pb isotope variations in leachate (blue) and detrital (grey) material from core site 712 along with multiproxy data of box core 712-1 (2–0 ka, light coloured curves, Spielhagen et al., 2011; Werner et al., 2011) and kastenlot core 712-2 (9–0.5 ka, dark coloured curves, Müller et al., 2012; Werner et al., 2013). **c**) Percentages of the subpolar planktic foraminifer species *T. quinqueloba* and the polar planktic foraminifer species *N. pachyderma*. **d**) Fluxes of ice-rafted material. **e**) Abundance of the sea ice indicating biomarker IP25 in kastenlot core 712-2. **f**) Planktic carbon isotope data measured on calcareous tests of *N. pachyderma*. **g**) Benthic oxygen isotope data measured on the benthic foraminifer species *Cibicidoides wuellerstorfi*. **h**) Age–depth-model and sedimentation rates in box core 712-1 (Spielhagen et al., 2011) and kastenlot core 712-2 (Müller et al., 2012), respectively. (For interpretation of the references to colour in this figure legend, the reader is referred to the web version of this article.)

slightly more radiogenic ε_{Nd} values is observed between 8.5 and 2.8 cal ka BP. Prior to 2.8 cal ka BP ε_{Nd} values between −10.6 and −10.0 are in good agreement with water column data from the present-day eastern Fram Strait and the Nordic Seas (ε_{Nd} values of −10.3 to −10.7; Piepgras and Wasserburg, 1987; Lacan and Jeandel, 2004b; Figs. 1b and 2). A shift occurred between 2.8 and 1.8 cal ka BP, after which ε_{Nd} reached significantly more radiogenic values between −9.1 and −8.8. One excursion to less radiogenic ε_{Nd} signatures (−10.2) was found for the sample at 2.75 cm core depth (ca 50 cal year BP/~1900 AD).

Measured core top ε_{Nd} values from the area match those obtained from downcore samples of station 712 during the past ca 2000 years. The core top samples had been stained with Rose Bengal onboard for foraminiferal investigations prior to isotope analysis. However, the consistence between core top and downcore data younger than 2 cal ka BP in core 712 (not stained with Rose Bengal), as well as near-seawater Sr isotope signatures of core top samples (Fig. 3) and the overprint by anthropogenic Pb (see below) support a reliable reflection of modern seawater Nd isotope values in the core top samples and demonstrate that the Rose Bengal did not cause a contamination.

Detrital Nd isotope signatures of the downcore record vary between −12.4 and −10.9 (Table 3, Fig. 4). A general trend to slightly more radiogenic ε_{Nd} values is also obvious in the detrital fraction between 8.5 and 2.8 cal ka BP. Prior to 2.8 cal ka BP ε_{Nd} values fluctuated around −12.1, whereas for the remainder of the record they were about 1 ε_{Nd} unit more radiogenic (−11.2).

Sediment coatings of the downcore record reveal a general trend to less radiogenic Pb isotope ratios since 8.5 cal ka BP (Figs. 4 and 5b). Prior to 1.0 cal ka BP, $^{206}Pb/^{204}Pb$ data were higher than the pre-anthropogenic value (ca 18.5) suggested by Gobeil et al. (2001) (Fig. 5). The shift to less radiogenic values around ca 1.6 cal ka BP (40 cm core depth) occurred more abruptly in the $^{207}Pb/^{204}Pb$ record (from 15.664 to 15.649) than the more gradual decreases of the $^{206}Pb/^{204}Pb$ and $^{208}Pb/^{204}Pb$ data (Fig. 4) at that time, which may indicate a change in source provenance. The marked decrease of all Pb isotope ratios at ca 1.0 cal ka BP suggests mixing of the unradiogenic anthropogenic Pb within the uppermost sediment layer via bioturbation (Fig. 4). These values are consistent with our core top data as well as core top data obtained from sediment leachates in the Arctic Ocean (Gobeil et al., 2001), both reflecting the input of anthropogenic Pb. Given that the anthropogenic Pb input started about 150 years ago, corresponding to a core depth of only 6 cm, the decrease in $^{206}Pb/^{204}Pb$ and other Pb isotope ratios clearly reflects a bioturbation mixing signal within at least the uppermost ca 15 cm. We note that our results agree with measurements of $^{206}Pb/^{204}Pb$ isotope composition from a sediment core from the same site (JM06-WP-04-MC, 78°54′N, 6°46′E) where a gradient between less radiogenic anthropogenic (18.483) and more radiogenic natural $^{206}Pb/^{204}Pb$ (18.930) was indicated within the uppermost ca 20 cm (Carignan et al., 2008). In Fig. 5b $^{206}Pb/^{204}Pb$ ratios are therefore shown without the uppermost 15 cm (i.e., the last ca 500 years). Noticeable is a trend to less radiogenic $^{206}Pb/^{204}Pb$ which already started at ca 3 cal ka BP, simultaneous to the approximate onset of the Late Holocene Neoglacial phase. Comparing our Holocene $^{206}Pb/^{204}Pb$ leachate data to those of core MC16 from eastern Fram Strait discussed by Maccali et al. (2012) proves difficult given that most of the relatively thin Holocene section (ca 15 cm) of core MC16 is strongly influenced by anthropogenic Pb.

Similar to the leachate data, all downcore Pb isotope ratios of the detrital fraction show a slight trend to less radiogenic values in the upper part of the studied section (Fig. 4) documenting anthropogenic contamination within the uppermost bioturbation-affected sediment layer ($^{206}Pb/^{204}Pb$ ~18.6). The detrital $^{206}Pb/^{204}Pb$ data shown in Fig. 5 (without the uppermost, contaminated section) reveal, however, relatively stable ratios around 19.05 and thus suggest no significant change of the sediment source throughout the Holocene. While a decreasing trend to significantly less radiogenic values (between 18.7 and 18.6) of detrital $^{206}Pb/^{204}Pb$ data in core MC16 points to a considerable effect of anthropogenic contamination within the Holocene part of core MC16 (Maccali et al., 2012), detrital $^{206}Pb/^{204}Pb$ data from core MC04 (Maccali et al., 2012) from the same site as our sediment core spanning the Late Holocene reveals similarly high radiogenic values between 18.9 and 19.0 for the uncontaminated sediment section below the uppermost bioturbation-affected sediment layer.

The $^{87}Sr/^{86}Sr$ signature was measured to support the seawater origin of the extracted Nd and Pb isotope signals from the ferromanganese coatings (Rutberg et al., 2000; Piotrowski et al., 2005; Gutjahr et al., 2007). All $^{87}Sr/^{86}Sr$ values from the leached fraction range between 0.70996 and 0.71174 (Figs. 3 and 4). Since Sr is a conservative element in seawater with a residence time of several million years (Palmer and Elderfield, 1985) the Sr isotope signature of the leachates should reflect the present-day seawater $^{87}Sr/^{86}Sr$ value of 0.70918 (Henderson et al., 1994). As ferromanganese oxyhydroxide coatings of both core top and downcore samples reveal slightly higher $^{87}Sr/^{86}Sr$ values than the present-day seawater, some dissolution of the detrital material has occurred during the Fe–Mn leaching process. This is consistent with findings from several sites from the North Atlantic where significant contributions of the detrital material to the Sr isotope signature of the leachates were observed (Piotrowski et al., 2004). By means of mass balance calculations, Gutjahr et al. (2007) showed that $^{87}Sr/^{86}Sr$ isotope compositions are often higher than the seawater Sr isotope composition but corresponding detrital contributions to the seawater Nd and Pb isotope compositions are at the same time insignificant and do not translate into altered seawater isotope compositions because the concentrations of Nd and Pb in the detrital material are much lower than those of Sr. We therefore infer reliable seawater-derived Nd and Pb isotope signals presented here, which is supported by the good match between seawater and coating data discussed before. An alternative explanation of the higher than seawater $^{87}Sr/^{86}Sr$ values is discussed below.

$^{87}Sr/^{86}Sr$ values of downcore detrital material are fluctuating between 0.7203 and 0.72385. Notably the detrital $^{87}Sr/^{86}Sr$ values of the two core top samples (0.73142 and 0.72549; Table 1, Fig. 3) are significantly higher than downcore $^{87}Sr/^{86}Sr$ values and may suggest a recent change of the detrital source area.

6. Discussion

6.1. Sedimentary Nd and Pb isotope data within a multiproxy context

The climatic and oceanographic development on the Western Svalbard margin during the past ca 9 cal ka BP has been discussed in detail in Müller et al. (2012) and Werner et al. (2013). The presented proxy record comprises the later part of the warm Early Holocene from ~9 cal ka BP onwards, as well as the Mid- and Late Holocene. In the following, we will briefly discuss the major trends of surface and bottom water variations at site 712 as derived from proxy indicators (Müller et al., 2012; Werner et al., 2013; Fig. 5) in relation to downcore variations of leachate and residual material in ε_{Nd} and $^{206}Pb/^{204}Pb$ during the past 9000 years. We note that the radiogenic isotope data is not as highly resolved as other proxy data studied in multidecadal resolution and allowing for a more detailed reconstruction of surface to deep water variability.

High proportions (up to >70%) of the subpolar planktic foraminiferal species *Turborotalita quinqueloba* (Fig. 5b) indicate strong Atlantic Water inflow into the Arctic during the Early and Mid-

Please cite this article in press as: Werner, K., et al., Neoglacial change in deep water exchange and increase of sea-ice transport through eastern Fram Strait: evidence from radiogenic isotopes, Quaternary Science Reviews (2013), http://dx.doi.org/10.1016/j.quascirev.2013.06.015

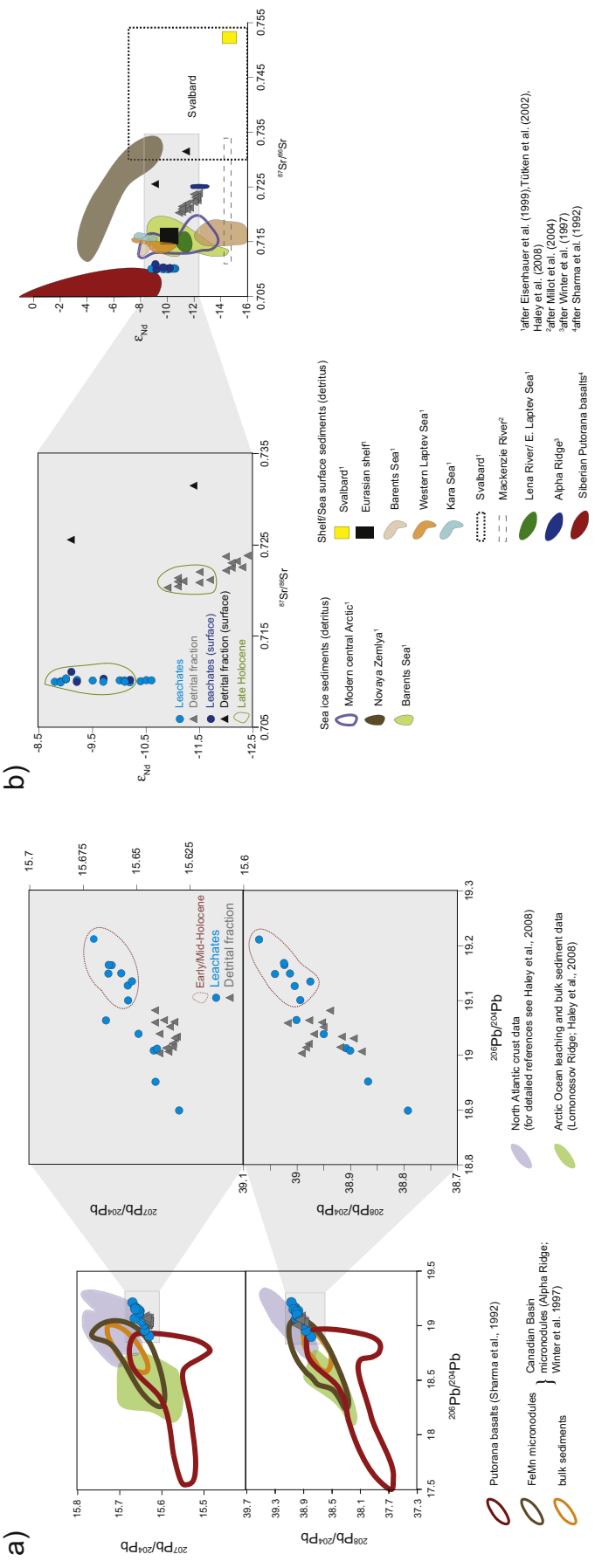

Fig. 6. a) Pb isotope leachate and detrital data compared to previously published data (after Haley et al., 2008b). b) Comparison between presented leachate and detrital data and compiled detrital data shown by Tütken et al. (2002), Haley et al. (2008b) and references therein, and Maccali et al. (2013) and references therein.

Holocene phases until ~5 cal ka BP. *T. quinqueloba* is one of the two dominant planktic foraminiferal species in eastern Fram Strait sediments and is indicative of Atlantic Water inflow in this area (Carstens et al., 1997; Volkmann, 2000). A sudden drop in *T. quinqueloba* percentages (<20%) and concurrent increase of percentages of the cold-water indicating planktic foraminifer species *Neogloboquadrina pachyderma* mark a significant weakening of inflowing AW masses and generally cooler surface water conditions after 5 cal ka BP, in response to decreasing insolation (Laskar et al., 2004). A summer cooling trend over the northern hemisphere continental landmasses and the North Atlantic Ocean during the second half of the Holocene was found in numerous reconstructions (e.g., Svendsen and Mangerud, 1997) and is discussed in more detail by Werner et al. (2013). Wanner et al. (2008) attributed this so-called Neoglacial cooling trend of the Late Holocene to decreasing solar radiation and a southward shift of the Intertropical Convergence Zone. In our record, this cooling is also documented by gradual increases of ice-rafted debris (IRD) contents and of accumulation rates of the sea-ice proxy IP25 (Müller et al., 2012; Fig. 5 d, e), which point to significantly higher sea-ice/iceberg abundance since the Mid-Holocene. Increasing sea-ice abundances in the Arctic and the Fram Strait since the Mid-Holocene were assigned to the Holocene sea level highstand at ca 5 cal ka BP (Bauch et al., 2001) and to associated flooding and initiation of similar-to-modern sea-ice production on the Siberian Arctic shelves (Werner et al., 2013).

A decrease in planktic $\delta^{13}C$ values during the past ca 3 cal ka BP (Fig. 5f) was ascribed to the density-controlled migration of planktic foraminifera (see Kozdon et al., 2009) into less-ventilated subsurface waters (Werner et al., 2013). In this case, decreasing planktic $\delta^{13}C$ values would be associated with a freshening of surface waters due to increased abundance of sea ice/icebergs during the Late Holocene Neoglacial phase.

In addition, after ca 3 cal ka BP benthic $\delta^{18}O$ values increased (Fig. 5g), which may either relate to a cooling of ca 1.4 °C or to increasing salinity by about 0.8 psu in bottom waters. Higher salinity of bottom waters is generated by dense water formation during winter sea-ice formation in southern and western Svalbard fjords (Quadfasel et al., 1988; Schauer, 1995; Rudels et al., 2005; Rasmussen and Thomsen, 2009). A salinity change of 0.8 in bottom water masses appears, however, unrealistic. Since the Nd isotope composition of shelf sediments and the bedrock of northern Svalbard is known to be less radiogenic (ε_{Nd} ~−14; Tütken et al., 2002; Andersson et al., 2008 and references therein; Fig. 1b), brine waters originating from southern or western Svalbard would probably lower the ε_{Nd} signal as they would have transported unradiogenic signatures to our study site. Instead, ε_{Nd} values of the past ca 2 cal ka BP reveal a trend to more radiogenic values both in the leachate and the detrital fraction. We therefore infer the increase in benthic oxygen isotope values to be indicative of a cooling of bottom water masses during the Late Holocene rather than variations in bottom water salinity.

Apart from the contaminated Pb isotopes within the uppermost sediment layer affected by bioturbation, the pattern of the Pb isotope data cannot clearly be related to the variations found in the proxy data shown in Fig. 5. Winter et al. (1997) and the works cited therein have reported the average $^{206}Pb/^{204}Pb$ isotope composition for the Caledonian Orogenic Belts of Greenland Scotland, Ireland, and Norway (which also includes Svalbard; Harland and Gayer, 1972) to range between 18.5 and 19.1. Thus, during the Early and Mid-Holocene the inflowing North Atlantic Drift waters may have been characterized by radiogenic $^{206}Pb/^{204}Pb$ values predominantly associated with the input of weathering material from the Western Svalbard continental margin. This can also be concluded from Fig. 6a, in which Early to Mid-Holocene Pb isotope leachate data plot close to Pb isotope compositions of North Atlantic continental crust (Haley et al., 2008b and references therein). However, radiogenic $^{206}Pb/^{204}Pb$ values up to 19.2 even exceed the range of 18.5 and 19.1 suggested by Winter et al. (1997) and may possibly be linked to Pb released by weathering of freshly eroded granitoids. Their values are often more radiogenic than those related to older soils due to the preferential release of the radiogenic Pb isotopes ^{206}Pb, ^{207}Pb, and ^{208}Pb as a consequence of α-recoil (Erel et al., 1994). Accordingly, Harlavan et al. (1998) showed that freshly weathered soil material on glacial moraines (both acid leachates and dissolved soil material) is characterized by more radiogenic Pb

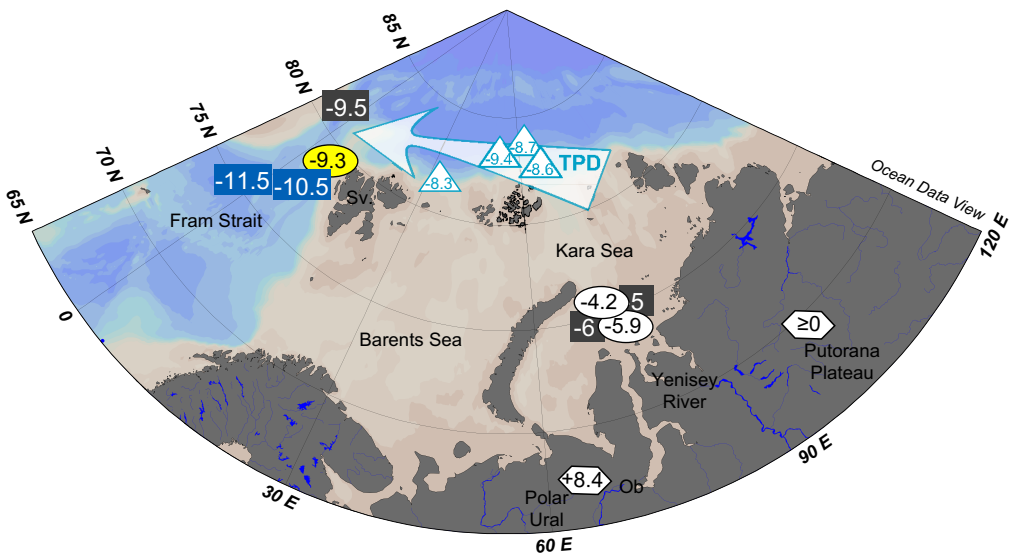

Fig. 7. Sea-ice drift from Kara Sea towards eastern Fram Strait (white arrow) after Pfirman et al. (1997). Included are ε_{Nd} values from the Kara Sea (seawater, grey squares: Porcelli et al., 2009; sediment leachates, white ovals: Chen et al., 2012; Haley and Polyak, 2013) and its source areas in Western Siberia (white hexagons; Edwards and Wasserburg, 1985; Sharma et al., 1992). Also shown are ε_{Nd} values from sea-ice sediments (detrital fraction) in the Barents Sea (white triangles with blue frame; Tütken et al., 2002) and from seawater (grey squares: Andersson et al., 2008, blue squares: this study) and sediment leachates in the Fram Strait (yellow oval: this study). (For interpretation of the references to colour in this figure legend, the reader is referred to the web version of this article.)

Please cite this article in press as: Werner, K., et al., Neoglacial change in deep water exchange and increase of sea-ice transport through eastern Fram Strait: evidence from radiogenic isotopes, Quaternary Science Reviews (2013), http://dx.doi.org/10.1016/j.quascirev.2013.06.015

isotope compositions whereas older soil material revealed less radiogenic Pb isotope values. During the warmer and probably wetter climate of the late Early and Mid-Holocene periods on Svalbard (e.g., Svendsen and Mangerud, 1997) chemical weathering processes were likely increased after the retreat of glacial ice coverage resulting in increased exposure of fresh and unweathered rocks that preferentially release radiogenic Pb during weathering. Part of this weathering material may have been released into Svalbard fjords by glacial and riverine transport and may therefore additionally account for the relatively radiogenic $^{206}Pb/^{204}Pb$ values during the Early Holocene phase.

6.2. Pathways of anthropogenic Pb to the eastern Fram Strait

Since atmospheric fluxes of Pb to the Arctic are low (Akeredolu et al., 1994; Hong et al., 1994), efficient delivery of contaminant Pb to polar basins is assumed to rather occur through oceanic transport (Alleman et al., 1999; Gobeil et al., 2001). Atlantic Water inflow to the Arctic Ocean via Fram Strait and the Barents Sea likely transported anthropogenic Pb produced by radionuclides from European nuclear fuel reprocessing plants discharged to the sea (Gobeil et al., 2001, and references therein). This pathway of contaminant Pb may also account for the unradiogenic Pb isotope compositions of our presented core top stations in the eastern Fram Strait. Surface sediments are located directly under the AW inflow and may be imprinted by the anthropogenic Pb signature arriving with the AW. On the other hand, it is also feasible that anthropogenic Pb produced by eastern European or Russian sources was transported to the eastern Fram Strait from northern Asia across the Arctic via the Transpolar Drift by sea ice (Gobeil et al., 2001).

6.3. Deepwater inflow to the eastern Fram Strait during the Holocene

Between 8.5 and 2.8 cal ka BP bottom water signatures obtained from the leachates reveal relatively unradiogenic ε_{Nd} values (−10.6 to −10.0). These values are indistinguishable from the seawater ε_{Nd} signatures of present-day deepwater in the Fram Strait and Nordic Seas (ε_{Nd} ~−10.5 to −11.9; Piepgras and Wasserburg, 1987; Lacan and Jeandel, 2004b; this study). From our multiproxy reconstruction we assume that prior to 5.2 cal ka BP the sea-ice margin was located north of our study site while between 5.2 and ~3 cal ka BP severe ice conditions lead to a location of the sea-ice margin south of our study site (see Werner et al., 2013). Both scenarios enable deepwater inflow from the Norwegian Sea which affects bottom sediments by seawater ε_{Nd} signatures of ~−10.5 to −11.9. Accordingly, we conclude that deepwater originating from the Norwegian Sea dominated the deeper waters in the eastern Fram Strait during the late Early to Mid-Holocene. This conclusion is consistent with seawater-derived ε_{Nd} values presented by Maccali et al. (2013) which varied between −11 and −10 during the Early to Mid-Holocene. It is furthermore supported by the Early to Mid-Holocene Pb isotope compositions similar to deep waters in the North Atlantic as revealed by ferromanganese crust data (Fig. 6a; Burton et al., 1997; O'Nions et al., 1998).

Maccali et al. (2013) have found a pattern similar to our data with slightly more radiogenic seawater ε_{Nd} data during the Late Holocene. The interpretation of the more radiogenic ε_{Nd} values (−8.8 to −9.1) after ca 2.8 cal ka BP turns out to be more complex with respect to Late Holocene changes of both surface and bottom water conditions. In the following, we provide a hypothesis for the possible cause of the considerable shift in leachate ε_{Nd} values during the Late Holocene Neoglacial period on the basis of a comparison to the high-resolution multiproxy data set of this Holocene sediment section (Müller et al., 2012; Werner et al., 2013).

6.4. Radiogenic isotope signatures in sea-ice sediments

For the Holocene period, Maccali et al. (2013) identified the Canadian margins and the Chukchi/East Siberian Seas as the predominant source regions of ice-rafted sediment supply to the central Fram Strait. However, the authors also noted that this situation might have changed very recently since their uppermost sample indicated a predominantly Siberian signature. They also supposed that a shift to more radiogenic seawater-derived ε_{Nd} data during the later Holocene may be linked to increasing influence of more radiogenic Pacific waters in the Fram Strait (Andersson et al., 2008). Our new seawater data from the eastern Fram Strait do, however, not confirm this assumption.

Today, seasonal sea ice formed on the shallow Siberian and North American shelves picks up lithic grains (Darby and Bischof, 2004) which are subsequently carried to the Fram Strait by the two major sea-ice drift pathways, the Transpolar Drift (TPD) and the Beaufort Gyre (BG) until released at the sea-ice margin upon melting (Pfirman et al., 1989). In particular, a large part of the sea ice formed on the Kara and Laptev Sea shelves is transported by the Siberian branch of the TPD across the Eurasian Basin and exits the Arctic Ocean through Fram Strait, thereby joining the East Greenland Current (Pfirman et al., 1989, 1997; Fig. 7). The Fram Strait thus today represents the main ablation area for Arctic sea ice (e.g., Kwok and Rothrock, 1999; Darby and Bischof, 2004; Cámara-Mor et al., 2010) where the warm Atlantic Water causes melting and release of sea-ice sediments year-round in the marginal ice zone of Fram Strait (e.g., Hebbeln and Wefer, 1991; Dethleff and Kuhlmann, 2010).

At present our study area is located in the zone of the widely fluctuating summer sea-ice margin in the eastern Fram Strait where warm Atlantic Water encounters cold surface waters and Arctic sea ice. Highest particle fluxes occur in the direct vicinity of the sea-ice margin (Hebbeln and Wefer, 1991) and ice-rafted material sinks down to accumulate and mix with current-transported fine-grained bottom sediments. Entrainment of sediments by sea ice mainly occurs along the shallow continental margins in the Arctic and is largely restricted to silt and clay-sized material, rarely containing grains larger than 0.1 mm (Nürnberg et al., 1994; Lisitzin, 2002; Darby, 2003; Dethleff and Kuhlmann, 2010). Accordingly, the sortable silt mean grain size fraction of sediments from the Yermak Plateau contains a significant amount of fine-grained ice-rafted material (Hass, 2002). In our record the coarse sediment fraction (250–1000 μm) only accounts for at maximum 1.7 weight% of the bulk sediment whereas the major part of sea-ice sediments is clearly fine-grained. In the following, we will therefore use the term 'ice-rafted fines' (IRF) for this fraction.

High sedimentation rates of 20–30 cm/1000 years found in our record for the past approximately 3000 years (Fig. 5h) have most likely been linked to enhanced release of sea-ice sediments associated with increased sea-ice abundance and a south-eastward shift of the marginal ice zone in the Fram Strait during the Late Holocene Neoglacial in response to post-glacial sea level rise and initiation of similar to modern sea-ice production (Dyke et al., 1997; Bauch et al., 1999; Prange and Lohmann, 2003; see also; Werner et al., 2013). Bacon et al. (1976) have determined the turnover time for particles in the mixed layer of the Atlantic Ocean to be on the order of one month. As yet there are no quantitative estimates on the duration of precipitation of early diagenetic ferromanganese coatings at the sediment water interface of marine sediments available. We therefore propose that for the Late Holocene during sinking the IRF material was exposed to the local Fram Strait seawater for only a relatively short period of time which may not have been sufficient to fully acquire the prevailing Nd isotope composition of the ambient bottom water.

Please cite this article in press as: Werner, K., et al., Neoglacial change in deep water exchange and increase of sea-ice transport through eastern Fram Strait: evidence from radiogenic isotopes, Quaternary Science Reviews (2013), http://dx.doi.org/10.1016/j.quascirev.2013.06.015

Although part of the ice-rafted material, in particular the coarser size fraction, is assumed to arrive from Svalbard glaciers (Werner et al., 2011) the majority of the IRF material was probably picked up by sea ice on the Siberian shelves and subsequently transported by the Transpolar Drift towards Fram Strait. We therefore hypothesize that the IRF grains acquired their ferromanganese coatings and seawater ε_{Nd} signature elsewhere, most probably already in the Arctic shelf seas. While the unradiogenic Nd isotope composition of the Mackenzie River (ε_{Nd} ~−13; Porcelli et al., 2009) rules out the Beaufort Gyre as a major source for IRF, significantly more radiogenic ε_{Nd} compositions were found on the Siberian shelves. Maccali et al. (2013) exclude a contribution of pre-formed (terrigeneous) oxides (Bayon et al., 2004) under glacial conditions. However, glacial conditions were markedly different from today (and supposedly from the Late Holocene) when riverine discharge of Yenisey and Ob Rivers into the Kara Sea is almost twice as large as the discharge of the Lena River into the Laptev Sea (ArcticRIMS, 2011). Today large amounts of particulate matter are transported onto the West Siberian shelves by rivers. Riverine input of the Yenisey and Ob Rivers contribute to highly radiogenic Nd isotope compositions to the Kara Sea seawater (ε_{Nd} ~−5.2 and −6.1, respectively; Porcelli et al., 2009) and were traced correspondingly in surface sediment leachates from the Kara Sea (Fig. 7; ε_{Nd} ~−5.9; Chen et al., 2012; ε_{Nd} ~−4.2; Haley and Polyak, 2013).

In combination with other available proxy data (Fig. 5) the Late Holocene shift to more radiogenic Nd leachate isotope data most likely indicates a south-eastward migration of the sea-ice margin to our study site in the eastern Fram Strait. We conclude that since ca 2.8 cal ka BP the marginal ice zone was located close to our study site where sea-ice sediments delivered by the Siberian branch of the TPD were released upon melting. A significant contribution of ice-rafted material from the Laptev and Kara Seas to Arctic Ocean and Fram Strait sediments had been proposed previously by e.g., Eisenhauer et al. (1999). By means of granulometric and mineralogical analyses, Dethleff and Kuhlmann (2010) showed that sea-ice sediments released in the eastern Fram Strait originate in particular from the Kara and western Laptev Seas. River waters and suspended matter have most likely been controlled by the same radiogenic sources within the catchment areas of Ob and Yenisey Rivers. The sources for the highly radiogenic sediment material include the Siberian Putorana basalts (e.g., Schoster et al., 2000; Stein et al., 2004) with radiogenic ε_{Nd} values ≥0 (Sharma et al., 1992) and the Polar Ural Mountains (ε_{Nd} ~+8.4; Edwards and Wasserburg, 1985). Pre-formed oxides with a highly radiogenic signature will thus form on sediment particles on the Kara Sea shelf. A significant fraction of the particulate material therefore probably obtains its particular pre-formed coatings and radiogenic ε_{Nd} signature on the Kara Sea shelf where the suspended matter is entrained by sea ice and transported towards Fram Strait by the TPD. A shift to more radiogenic material is also obvious in the detrital material of the sediment core. This suggests a change in its source area since the Late Holocene. However, since the sediments in the eastern Fram Strait still reveal ε_{Nd} values between −11.5 and −11 during the Late Holocene the sediment signatures must be a mixture of several sources. More radiogenic IRF material from the Siberian shelves has likely been mixed and diluted with less radiogenic sediment material in the Fram Strait. Our hypothesis is corroborated by the reported sea-ice pathway from the Kara Sea to the eastern Fram Strait by Pfirman et al. (1997) and coincides with radiogenic Nd isotope composition of −9.4 to −8.3 in the detrital fraction of sea-ice sediments en route in the Barents Sea (Tütken et al., 2002; Figs. 6b and 7). Also, the Late Holocene leachate Pb data which plot within the area of Putorana basalts (Fig. 6a) point to a significant contribution of this Siberian source of sediment coatings. Local contamination of authigenic oxyhydroxides by preformed riverine Fe–Mn oxides on detrital material has been reported previously close to the west African margin (Bayon et al., 2004). Andersson et al. (2008) noted that Nd derived from river water input can also be transported offshore and at a later stage influence the isotopic composition of the deeper waters. However, for the shallow Siberian shelves we propose a sea-ice related particulate transport of radiogenic ε_{Nd} values to the Arctic Ocean and the Fram Strait. Transport of particles with preformed coatings may also have contributed to the Nd isotope ratios found in sediment coatings near the North Pole during glacial periods after 2 Ma (Haley et al., 2008a,b).

6.5. Paleoclimatic implications

The shift to more radiogenic ε_{Nd} signature of the leachates after ~2.8 cal ka BP indicates a position of the sea-ice margin near our study site. From proxy data, Werner et al. (2013) reconstructed a major shift to colder Neoglacial conditions at 5.2 cal ka BP caused by the onset of similar to modern sea-ice production and export via Fram Strait as a consequence of the Holocene sea-level highstand at that time (Bauch et al., 2001). In addition, perennial sea-ice conditions between ~5.2 and ~3 cal ka BP were found and a location of the sea-ice margin south of the study site was assumed for that period of time. Deepwater inflow from the Norwegian Sea with seawater ε_{Nd} signatures of ~−11.9 to −10.5 was therefore the major source for Nd isotope signatures stored in the oxyhydroxide coatings of bottom sediments at that time.

These conditions changed at ~3 cal ka as deduced from increased percentages of the subpolar planktic foraminiferal species *T. quinqueloba*, which point to increased inflow of Atlantic Water through eastern Fram Strait (Werner et al., 2013). A strengthening of AW inflow which is consistent with data from south of Svalbard (Sarnthein et al., 2003; Rasmussen et al., 2007) led to a slight northwest retreat of the sea-ice margin at 3 cal ka to site 712 in the eastern Fram Strait and a position of the sea-ice margin similar to today for the remainder of the record. We thus conclude that the more radiogenic ε_{Nd} signatures obtained from the leachates (−8.8 to −9.1) for the past 3 cal ka do not represent pure seawater signatures but were caused by increased admixture of sea-ice rafted fine-grained material originating from the Kara and Barents Sea shelves to the bottom sediments at that time.

Prior to the significant shift at 2.8 cal ka BP, two outliers of higher radiogenic ε_{Nd} values at 5.2 and 3.3 cal ka BP (−9.7 and −9.5, respectively) were identified. Despite the fact that these excursions are barely significant, they may correspond to earlier migrations of the sea-ice margin to the site.

The less radiogenic ε_{Nd} signature (−10.15) in the sample from 2.75 cm (Fig. 4) clearly differs from more radiogenic values (−9.1 to −8.8) in the uppermost ca 40 cm of the studied core section. Although the overall bioturbation mixing depth covers at least the uppermost ca 15 cm of the sediment core as was shown by anthropogenic Pb impact (see above), the less radiogenic ε_{Nd} signature at 2.75 cm did apparently not affect adjacent samples at 0 and 10.25 cm. Thus, we assume that bioturbation mixing may not have been effective enough to completely homogenize the bioturbated sediment layer. The measured ε_{Nd} signal of −10.15 in the sample from 2.75 cm displays a seawater signature found in the Nordic Seas (Lacan and Jeandel, 2004b; Andersson et al., 2008 and references therein). According to the age model (Spielhagen et al., 2011) the core depth of 2.75 cm corresponds to an age of ~1910 AD. Werner et al. (2011) have shown that very cold conditions affected the surface water layers in the eastern Fram Strait well into the 20th century which were likely associated with the final stages of the Little Ice Age (LIA). Thus, the relatively unradiogenic ε_{Nd}

Please cite this article in press as: Werner, K., et al., Neoglacial change in deep water exchange and increase of sea-ice transport through eastern Fram Strait: evidence from radiogenic isotopes, Quaternary Science Reviews (2013), http://dx.doi.org/10.1016/j.quascirev.2013.06.015

signal of −10.15 found at site 712 may have been produced by inflowing AW or NSDW during a time when the sea-ice margin advanced to a position south of our study site. As a consequence, the IRF particle load transported by the Arctic sea ice was released further south while our study site was not affected by IRF release during this time. Instead of a major IRF input to bottom sediments as during most of the Late Holocene when the sea-ice margin fluctuated between locations very close to our study site, bottom sediments rather acquired the less radiogenic seawater ε_{Nd} by the inflowing AW and NSDW derived from North Atlantic Drift waters under permanent sea-ice coverage near 1900 AD.

7. Conclusions

Core top and modern water samples obtained from the West Spitsbergen continental margin were investigated for their seawater-derived radiogenic Nd compositions to calibrate the sediment data to present-day bottom water distributions. On the basis of this calibration a Nd and Pb isotope record (leachate and detrital fraction) of core MSM5/5-712 in the eastern Fram Strait covering the past ca 8.5 cal ka BP has been established, which is compared to information from a multiproxy data set reflecting changes in environmental conditions obtained for the same core.

Surface samples consistently display a relatively radiogenic Nd isotope signature (∼−9) different from modern seawater ε_{Nd} values in the area (−11.9 to −10.1; Lacan and Jeandel, 2004b; Andersson et al., 2008 and references therein; this study). Today, the Fram Strait area is primarily influenced by the inflow of North Atlantic Drift Waters and Norwegian Sea Deep Water mainly produced in the Nordic Seas. A corresponding Nd isotope composition (−10.6 to −10.1) found in the downcore seawater record prior to 2.8 cal ka BP can thus clearly be related to the dominant advection of deep waters from the Nordic Seas.

After ca 2.8 cal ka BP ε_{Nd} values increased to −9.1 and −8.8, comparable to the core top sample signatures. Since the Fram Strait acts as a major ablation area for ice-rafted material entrained by Arctic sea ice and delivered by the Transpolar Drift we hypothesize that fine-grained sea-ice material with pre-formed, more radiogenic ε_{Nd} signatures has been transported by the TPD to eastern Fram Strait during the Late Holocene due to a south-eastward migration of the marginal ice zone. There, melting led to rapid burial and probably storage of the sediment material which had acquired its radiogenic ε_{Nd} values elsewhere on the shallow Siberian shelves. With this study we demonstrate that Nd isotope data are applicable to revealing shifts of the sea-ice margin in the eastern Fram Strait.

A potential source area for the more radiogenic ε_{Nd} values in ice-rafted material is the Kara Sea shelf where seawater-derived Nd isotope compositions of both seawater and oxyhydroxide coatings of sediment leachates reveal radiogenic values between −6.1 and −3.4 (Porcelli et al., 2009; Chen et al., 2012). Proxy data from the core site (Werner et al., 2011, 2013; Müller et al., 2012) indicate that the shift to higher ε_{Nd} values observed after ca 2.8 cal ka BP was accompanied by a cooling of surface and bottom waters and a marked increase in ice-rafted fine material since approximately 3 cal ka BP.

Pb isotope composition of Early to Mid-Holocene samples (leachate and detrital material) plot close to the signature of North Atlantic waters as reconstructed from ferromanganese crust data. Relatively radiogenic Pb isotope signatures in the late Early and Mid-Holocene point to a dominance of contributions from source rocks in the Caledonian Orogenic Belts of Greenland, Scotland, and Ireland. In addition, increased chemical weathering of postglacially freshly exposed granitic rocks most likely contributed to somewhat more radiogenic Pb isotope ratios in seawater during the late Early to Mid-Holocene.

Acknowledgements

The German Research Foundation (DFG) provided financial support of K. Werner within the Priority Programme 1266 (INTERDYNAMIC, project HOVAG). For retrieving the water samples onboard RV “Polarstern” during cruise leg ARK-XXVI/1 we kindly thank the crew and science party (in particular Maciej Telesinski). For providing Nd concentration data and thorough instructions and advice in the laboratory we are grateful to Moritz Zieringer and Ed Hathorne. We thank Roland Stumpf, Dorothea Bauch, and Torben Struve for valuable comments and discussions. We wish to thank the science party and crew onboard RV “Maria S. Merian” during the expedition MSM5/5 for retrieving the sediment material. We are grateful to the two anonymous reviewers for providing constructive comments on the manuscript.

References

Aagaard, K., Swift, J.H., Carmack, E.C., 1985. Thermohaline circulation in the Arctic Mediterranean Seas. Journal of Geophysical Research 90, 4833–4846.
Aagaard, K., Foldwik, A., Hillman, S.R., 1987. The West Spitsbergen Current: disposition and water mass transformation. Journal of Geophysical Research 92, 3778–3784.
Aagaard, K., Fahrbach, E., Meincke, J., Swift, J.H., 1991. Saline outflow from the Arctic Ocean: its contribution to the deep waters of the Greenland, Norwegian, and Iceland Seas. Journal of Geophysical Research 96, 20,433–20,441.
Aagaard, K., Carmack, E.C., 1989. The role of sea ice and other fresh water in the Arctic Circulation. Journal of Geophysical Research 94, 14,485–14,498.
Abouchami, W., Galer, S.J.G., Koschinsky, A., 1999. Pb and Nd isotopes in NE Atlantic Fe-Mn crust: proxies for trace metal paleosources and paleocean circulation. Geochimica et Cosmochimica Acta 63, 1489–1505.
Albarède, F., Telouk, P., Blichert-Toft, J., Boyet, M., Agranier, A., Nelson, B., 2004. Precise and accurate isotopic measurements using multiple-collector ICPMS. Geochimica et Cosmochimica Acta 68, 2725–2744.
Alleman, L.Y., Véron, A.J., Church, T.M., Flegal, A.R., Hamelin, B., 1999. Invasion of the abyssal North Atlantic by modern anthropogenic lead. Geophysical Research Letters 26, 1477–1480.
Akeredolu, F.A., Barrie, L.A., Olson, M.P., Oikawa, K.K., Pacyna, J.M., Keeler, G.J., 1994. The flux of anthropogenic trace metals into the arctic from the mid-latitudes in 1979/80. Atmospheric Environment 28, 1557–1572.
Amakawa, H., Sasaki, K., Ebihara, M., 2009. Nd isotopic composition in the central North Pacific. Geochimica et Cosmochimica Acta 73, 4705–4719.
Anderson, L.G., Jones, E.P., Rudels, B., 1999. Ventilation of the Arctic Ocean estimated by a plume entrainment model constrained by CFCs. Journal of Geophysical Research 104, 13423–13429.
Andersson, P.S., Porcelli, D., Frank, M., Björk, G., Dahlqvist, R., Gustafsson, Ö., 2008. Neodymium isotopes in seawater from the Barents Sea and Fram Strait Arctic-Atlantic gateways. Geochimica et Cosmochimica Acta 72, 2854–2867.
ArcticRIMS Database/R-ArcticNet (v4.0), 2011. A Regional, Hydrometeorological Data Network for the Pan-Arctic Region. http://rims.unh.edu/.
Arsouze, T., Dutay, J.-C., Lacan, F., Jeandel, C., 2009. Reconstructing the Nd oceanic cycle using a coupled dynamical-biogeochemical model. Biogeosciences 6, 5549–5588.
Bacon, M.P., Spencer, D.W., Brewer, P.G., 1976. ^{210}PB/^{226}Ra and ^{210}Po/^{210}Pb disequilibria in seawater and suspended particulate matter. Earth and Planetary Science Letters 32, 277–296.
Barrat, J.A., Keller, F., Amossé, J., 1996. Determination of rare earth elements in sixteen silicate reference samples by ICP-MS after Tm addition and ion exchange separation. Geostandard Newsletter 20, 133–139.
Bauch, D., Schlosser, P., Fairbanks, R.G., 1995. Freshwater balance and the sources of deep and bottom waters in the Arctic Ocean inferred from the distribution of $H_2{}^{18}O$. Progress in Oceanography 35, 53–80.
Bauch, H.A., Kassens, H., Erlenkeuser, H., Grootes, P.M., Thiede, J., 1999. Depositional environment of the Laptev Sea (Arctic Siberia) during the Holocene. Boreas 28, 194–204.
Bauch, H.A., Mueller-Lupp, T., Taldenkova, E., Spielhagen, R.F., Kassens, H., Grootes, P.M., Thiede, J., Heinemeier, J., Petryashov, V.V., 2001. Chronology of the Holocene transgression at the North Siberian margin. Global and Planetary Change 31, 125–139.
Bayon, G., German, C.R., Boella, R.M., Milton, J.A., Taylor, R.N., Nesbitt, R.W., 2002. An improved method for extracting marine sediment fractions and its application to Sr and Nd isotopic analysis. Chemical Geology 187, 179–199.
Bayon, G., German, C.R., Burton, K.W., Nesbitt, R.W., Rogers, N., 2004. Sedimentary Fe-Mn oxyhydroxides as paleoceanographic archives and the role of Aeolian flux in regulation oceanic dissolved REE. Earth and Planetary Science Letters 224, 477–492.
Beszczynska-Möller, A., Wisotzki, A., 2012. Physical Oceanography During POLARSTERN Cruise ARK-XVI/1. Alfred Wegener Institute for Polar and Marine Research, Bremerhaven. http://dx.doi.org/10.1594/PANGAEA.774196.

Please cite this article in press as: Werner, K., et al., Neoglacial change in deep water exchange and increase of sea-ice transport through eastern Fram Strait: evidence from radiogenic isotopes, Quaternary Science Reviews (2013), http://dx.doi.org/10.1016/j.quascirev.2013.06.015

Björk, G., Anderson, L.G., Jakobsson, M., Antony, D., Eriksson, B., Eriksson, P.B., Hell, B., Hjalmarsson, S., Janzen, T., Jutterström, S., Linders, J., Löwemark, L., Marcussen, C., Olsson, K.A., Rudels, B., Sellén, E., Sølvsten, M., 2010. Flow of Canadian basin deep water in the Western Eurasian Basin of the Arctic Ocean. Deep-Sea Research I 57, 577–586.
Broecker, W.S., 1982. Ocean chemistry during glacial time. Geochimica et Cosmochimica Acta 46, 1689–1705.
Broecker, W.S., 1991. The great ocean conveyor. Oceanography 4, 79–89.
Budéus, G., Ronski, S., 2009. An integral view of the hydrographic development in the Greenland Sea over a decade. The Open Oceanography Journal 3, 8–39.
Burton, K.W., Ling, H.-F., O'Nions, R.K., 1997. Closure of the Central American Isthmus and its effect on deep-water formation in the North-Atlantic. Nature 386, 382–385.
Cámara-Mor, P., Masqué, P., Garcia-Orellana, J., Cochran, J.K., Mas, J.L., Chamizo, E., Hanfland, C., 2010. Arctic Ocean sea ice drift origin derived from artificial radionuclides. Science of the Total Environment 408, 2249–3358.
Carignan, J., Hillaire-Marcel, C., de Vernal, A., 2008. Arctic vs. North Atlantic water mass exchanges in Fram Strait from Pb isotopes in sediments. Canadian Journal of Earth Sciences 45, 1253–1263.
Carstens, J., Hebbeln, D., Wefer, G., 1997. Distribution of planktic foraminifera at the ice margin in the Arctic (Fram Strait). Marine Micropaleontology 29, 257–269.
Chen, T.-Y., Frank, M., Haley, B.A., Gutjahr, M., Spielhagen, R.F., 2012. Variations of North Atlantic inflow to the central Arctic Ocean over the last 14 million years inferred from hafnium and neodymium isotopes. Earth and Planetary Science Letters 353–354, 82–92.
Cohen, A.S., O'Nions, R.K., Siegenthaler, R., Griffin, W.L., 1988. Chronology of the pressure-temperature history recorded by a granulite terrain. Contributions to Mineralogy and Petrology 98, 303–311.
Crocket, K.C., Vance, D., Gutjahr, M., Foster, G.L., Richards, D.A., 2011. Persistent Nordic deep-water overflow to the glacial North Atlantic. Geology 39, 515–518.
Dahlqvist, R., Andersson, P.S., Porcelli, D., 2007. Nd isotopes in Bering Strait and Chukchi water. Geochimica et Cosmochimica Acta 71, A196.
Darby, D.A., 2003. Sources of sediment found in the sea ice from the western Arctic Ocean, new insights into processes of entrainment and drift patterns. Journal of Geophysical Research 108 (C8), 3257.
Darby, D.A., Bischof, J.F., 2004. A Holocene record of changing Arctic Ocean ice drift analogous to the effects of the Arctic Oscillation. Paleoceanography 19, PA1027.
Dethleff, D., Kuhlmann, G., 2010. Fram Strait sea-ice sediment provinces based on silt and clay compositions identify Siberian Kara and Laptev seas as main source regions. Polar Research 29, 265–282.
Dyke, A.S., England, J., Reimnitz, E., Jette, J., 1997. Changes in driftwood delivery to the Canadian Arctic Archipelago: the hypothesis of postglacial oscillations of the transpolar drift. Arctic 50, 1–16.
Edwards, R.L., Wasserburg, G.J., 1985. The age and emplacement of obducted oceanic crust in the Urals from Sm-Nd and Rb-Sr systematics. Earth and Planetary Science Letters 72, 389–404.
Eisenhauer, A., Meyer, H., Rachold, V., Tütken, T., Wiegand, B., Hansen, B.T., Spielhagen, R.F., Lindeman, F., Kassens, H., 1999. Grain size separation and sediment mixing in Arctic Ocean sediments: evidence from the strontium isotope systematic. Chemical Geology 158, 173–188.
Erel, Y., Harlavan, Y., Blum, J.D., 1994. Lead isotope systematics of granitoid weathering. Geochimica et Cosmochimica Acta 58, 5299–5306.
Falck, E., Kattner, G., Budéus, G., 2005. Disappearance of Pacific Water in the northwestern Fram Strait. Geophysical Research Letters 32, L14619.
Frank, M., 2002. Radiogenic isotopes: tracers of past ocean circulation and erosional input. Reviews of Geophysics 40 (1), 1001.
Galer, S.J.G., O'Nions, R.K., 1989. Chemical and isotopic studies of ultramafic inclusions from the San Carlos volcanic field, Arizona: a bearing on their petrogenesis. Journal of Petrology 30, 1033–1064.
Gobeil, C., Macdonald, R.W., Smith, J.N., Beaudin, L., 2001. Atlantic water flow pathways revealed by lead contamination in Arctic basin sediments. Science 293, 1301–1304.
Gutjahr, M., Frank, M., Stirling, C.H., Klemm, V., van de Flierdt, T., Halliday, A.N., 2007. Reliable extraction of a deepwater trace metal isotope signal from Fe-Mn oxyhydroxide coatings of marine sediments. Chemical Geology 242, 351–370.
Hald, M., Ebbesen, H., Forwick, M., Godtliebsen, F., Khomenko, L., Korsun, S., Ringstadt Olsen, L., Vorren, T.O., 2004. Holocene paleoceanography and glacial history of the West Spitsbergen area, Euro-Arctic margin. Quaternary Science Reviews 23, 2075–2088.
Hald, M., Andersson, C., Ebbesen, H., Jansen, E., Klitgaard-Kristensen, D., Risebrobakken, B., Salomonsen, G.R., Sarnthein, M., Sejrup, H.P., Telford, R.J., 2007. Variations in temperature and extent of Atlantic water in the northern North Atlantic during the Holocene. Quaternary Science Reviews 26, 3423–3440.
Haley, B., Polyak, L., 2013. Pre-modern Arctic Ocean circulation from surface sediment neodymium isotopes. Geophysical Research Letters 40 (5), 893–897.
Haley, B., Frank, M., Spielhagen, R.F., Eisenhauer, A., 2008a. Influence of brine formation on Arctic Ocean circulation over the past 15 million years. Nature Geoscience 1, 68–72.
Haley, B., Frank, M., Spielhagen, R.F., Fietzke, J., 2008b. Radiogenic isotope record of Arctic Ocean circulation and weathering inputs of the past 15 million years. Paleoceanography 23, PA1S13.
Hamelin, B., Grousset, F., Sholkovitz, E.R., 1990. Pb isotopes in surficial pelagic sediments from the North Atlantic. Geochimica et Cosmochimica Acta 54, 37–47.
Harland, W.B., Gayer, R.A., 1972. The Arctic Caledonides and earlier oceans. Geological Magazine 109, 289–314.
Harlavan, Y., Erel, Y., Blum, J.D., 1998. Systematic changes in lead isotopic composition with soil age in glacial granitic terrains. Geochimica et Cosmochimica Acta 62, 33–46.
Hass, H.C., 2002. A method to reduce the influence of ice-rated debris on a grain size record from northern Fram Strait, Arctic Ocean. Polar Research 21, 299–306.
Hebbeln, D., Wefer, G., 1991. Effects of ice coverage and ice-rafted material on sedimentation in the Fram Strait. Nature 350, 409–411.
Henderson, G.M., Martel, D.M., Onions, R.K., Shackleton, N.J., 1994. Evolution of seawater Sr-87/Sr-86 over the last 400 ka – the absence of glacial-interglacial cycles. Earth and Planetary Science Letters 128 (3–4), 643–651.
Holland, M.M., Bitz, C.M., Eby, M., Weaver, A.J., 2001. The role of ice-ocean interactions in the variability of the North Atlantic thermohaline circulation. Journal of Climate 14, 656–675.
Hong, S., Candelone, J.-P., Patterson, C.C., Boutron, C.F., 1994. Greenland ice evidence of hemispheric lead pollution two millennia ago by Greek and Roman civilizations. Science 265, 1841–1843.
Horwitz, E.P., Chiarizia, R., Dietz, M.L., 1992. A novel strontium-selective extraction chromatographic resin. Solvent Extraction and Ion Exchange 10, 313–336.
Jacobsen, S.B., Wasserburg, G.J., 1980. Sm-Nd isotopic evolution of chondrites. Earth and Planetary Science Letters 50, 139–155.
Jakobsson, M., Mayer, L., Coakley, B., Dowdeswell, J.A., Forbes, S., Fridman, B., Hodnesdal, H., Noormets, R., Pedersen, R., Rebesco, M., Schenke, H.W., Zarayskaya, Y., Accettella, D., Armstrong, A., Anderson, R.M., Bienhoff, P., Camerlenghi, A., Church, I., Edwards, M., Gardner, J.V., Hall, J.K., Hell, B., Hestvik, O., Kristoffersen, Y., Marcussen, C., Mohammad, R., Mosher, D., Nghiem, S.V., Pedrosa, M.T., Travaglini, P.G., Weatherall, P., 2012. The International Bathymetric Chart of the Arctic Ocean (IBCAO) version 3.0. Geophysical Research Letters 39, L12609.
Jang, K., Han, Y., Huh, Y., Nam, S.-I., Stein, R., Mackensen, A., Matthiessen, J., 2013. Glacial freshwater discharge events recorded by authigenic neodymium isotopes in sediments from the Mendeleev Ridge, western Arctic Ocean. Earth and Planetary Science Letters 369–370, 148–157.
Johannessen, O.M., 1986. Brief overview of the physical oceanography. In: Hurdle, B.G. (Ed.), The Nordic Seas. Springer, New York, pp. 103–127.
Johansson, Å., Gee, D.G., 1999. The late Palaeproterozoic Eskolabreen granitoids of southern Ny Friesland, Svalbard Caledonides – geochemistry, age, and origin. GFF 121, 113–126.
Johansson, Å., Larionov, A.N., Tebenkov, A.M., Ohta, Y., Gee, D.G., 2002. Caledonian granites of western and central Nordaustlandet, northeast Svalbard. GFF 124, 135–148.
Jones, E.P., 2001. Circulation in the Arctic Ocean. Polar Research 20, 139–146.
Jones, E.P., Rudels, B., Anderson, L.G., 1995. Deep waters of the Arctic Ocean: origins and circulation. Deep Sea Research I 42, 737–760.
Jones, E.P., Swift, J.H., Anderson, L.G., Lipizer, M., Civitarese, G., Falkner, K.K., Kattner, G., McLaughlin, F., 2003. Tracing Pacific water in the North Atlantic Ocean. Journal of Geophysical Research 108, 3116.
Karcher, M.J., Gerdes, R., Kauker, F., Köberle, C., 2003. Arctic warming: Evolution and spreading of the 1990s warm event in the Nordic seas and the Arctic Ocean. Journal of Geophysical Research 108, 3034.
Kozdon, R., Eisenhauer, A., Weinelt, M., Meland, M.Y., Nürnberg, D., 2009. Reassessing Mg/Ca temperature calibrations of *Neogloboquadrina pachyderma* (sinistral) using paired $\delta^{44/40}$ and Mg/Ca measurements. Geochemistry, Geophysics, Geosystems 10 (3), Q03005.
Kwok, R., Rothrock, D.A., 1999. Variability of Fram Strait ice flux and North Atlantic oscillation. Journal of Geophysical Research 104, 5177–5189.
Lacan, F., Jeandel, C., 2004a. Denmark Strait water circulation traced by heterogeneity in neodymium isotopic compositions. Deep-Sea Research I 51, 71–82.
Lacan, F., Jeandel, C., 2004b. Neodymium isotopic composition and rare earth element concentrations in the deep and intermediate Nordic Seas: constraints on the Iceland Scotland overflow water signature. Geochemistry, Geophysics, Geosystems 5, Q11006.
Lacan, F., Jeandel, C., 2005. Neodymium isotopes as a new tool for quantifying exchange fluxes at the continent-ocean interface. Earth and Planetary Science Letters 232, 245–257.
Laskar, J., Robutel, P., Joutel, F., Gastineau, M., Correia, A.C.M., Levrard, B., 2004. A long-term numerical solution for the insolation quantities of the Earth. Astronomy & Astrophysics 428, 261–285.
Le Fèvre, B., Pin, C., 2005. A straightforward separation scheme for concomitant Lu-Hf and Sm-Nd isotope ratio and isotope dilution analysis. Analytica Chimica Acta 543, 209–221.
Lisitzin, A.P., 2002. Sea-ice and Iceberg Sedimentation in the Ocean – Recent and Past. Springer-Verlag, Berlin, p. 563.
Lohmann, G., Gerdes, R., 1998. Sea ice effects on the sensitivity of the thermohaline circulation. Journal of Climate 11, 2789–2803.
Lugmair, G.W., Galer, S.J.G., 1992. Age and isotopic relationships among the angrites Lewis Cliff 86010 and Angra dos Reis. Geochimica et Cosmochimica Acta 56, 1673–1694.
Maccali, J., Hillaire-Marcel, C., Carignan, J., Reisberg, L.C., 2012. Pb isotopes and geochemical monitoring of Arctic sedimentary supplies and water mass export through Fram Strait since the Last Glacial Maximum. Paleoceanography 97, PA1201.
Maccali, J., Hillaire-Marcel, C., Carignan, J., Reisberg, L.C., 2013. Geochemical signatures of sediments documenting Arctic sea-ice and water mass export

Please cite this article in press as: Werner, K., et al., Neoglacial change in deep water exchange and increase of sea-ice transport through eastern Fram Strait: evidence from radiogenic isotopes, Quaternary Science Reviews (2013), http://dx.doi.org/10.1016/j.quascirev.2013.06.015

through Fram Strait since the Last Glacial Maximum. Quaternary Science Reviews 64, 136–151.
Marnela, M., Rudels, B., Olsson, K.A., Anderson, L.G., Jeansson, E., Torres, D.J., Messias, M.-J., Swift, J.H., Watson, A.J., 2008. Transports of Nordic Seas water masses and excess SF_6 through Fram Strait to the Arctic Ocean. Progress in Oceanography 78, 1–11.
Mauritzen, C., 1996. Production of dense overflow waters feeding the North Atlantic across the Greenland-Scotland Ridge. Part 1: evidence for a revised circulation scheme. Deep-Sea Research 43, 769–806.
Mauritzen, C., Häkkinen, S., 1997. Influence of sea ice on the thermohaline circulation in the Arctic-North Atlantic Ocean. Geophysical Research Letters 24, 3257–3260.
Müller, J., Werner, K., Stein, R., Fahl, K., Moros, M., Jansen, E., 2012. Holocene cooling culminates in Neoglacial sea ice oscillations in Fram Strait. Quaternary Science Reviews 47, 1–14.
Nørgaard-Pedersen, N., Spielhagen, R.F., Erlenkeuser, H., Grootes, P.M., Heinemeier, J., Knies, J., 2003. Arctic Ocean during the Last Glacial Maximum: Atlantic and polar domains of surface water mass distribution and ice cover. Paleoceanography 18, 1063.
Nürnberg, D., Wollenburg, I., Dethleff, D., Eicken, H., Kassens, H., Letzig, T., Reimnitz, E., Thiede, J., 1994. Sediments in Arctic sea ice: implications for entrainment, transport and release. Marine Geology 119, 185–214.
O'Nions, R.K., Frank, M., von Blanckenburg, F., Ling, H.-F., 1998. Secular variation of Nd and Pb-isotopes in ferromanganese crusts from the Atlantic, Indian and Pacific Oceans. Earth and Planetary Science Letters 155, 15–28.
Palmer, M.R., Elderfield, H., 1985. Sr isotope composition of seawater over the past 75 Myr. Nature 314, 526–528.
Peucat, J.J., Ohta, Y., Gee, D.G., Bernard-Griffith, J., 1989. U-Pb, Sr and Nd evidence for Grenivillan and latest Proterozoic tectonothermal activity in the Spitsbergen Caldonides, Arctic Ocean. Lithos 22, 275–285.
Pfirman, S., Gascard, J.-C., Wollenburg, I., Mudie, P., Abelmann, A., 1989. Particle-laden Eurasian Arctic sea ice: observations from July and August 1987. Polar Research 7, 59–66.
Pfirman, S., Colony, R., Nürnberg, D., Eicken, H., Rigor, I., 1997. Reconstructing the origin and trajectory of drifting Arctic sea ice. Journal of Geophysical Research 102, 12,575–12,586.
Piepgras, D.J., Jacobsen, S.B., 1988. The isotopic composition of neodymium in the North Pacific. Geochimica et Cosmochimica Acta 52, 1373–1381.
Piepgras, D.J., Wasserburg, G.J., 1980. Neodymium isotopic variations in seawater. Earth and Planetary Science Letters 50, 128–138.
Piepgras, D.J., Wasserburg, G.J., 1987. Rare earth element transport in the western North Atlantic inferred from Nd isotopic observations. Geochimica et Cosmochimica Acta 51, 1257–1271.
Piotrowski, A.M., Goldstein, S.L., Hemming, S.R., Fairbanks, R.G., 2004. Intensification and variability of ocean thermohaline circulation through the last deglaciation. Earth and Planetary Science Letters 225, 205–220.
Piotrowski, A.M., Goldstein, S.L., Hemming, S.R., Fairbanks, R.G., 2005. Temporal relationships of carbon cycle and ocean circulation at glacial boundaries. Science 307, 1933–1938.
Porcelli, D., Andersson, P.S., Baskaran, M., Frank, M., Björk, G., Semiletov, I., 2009. The distribution of neodymium isotopes in Arctic Ocean basins. Geochimica et Cosmochimica Acta 73, 2645–2659.
Prange, M., Lohmann, G., 2003. Effects of mid-Holocene river runoff on the Arctic ocean/sea-ice system: a numerical study. The Holocene 13, 335–342.
Quadfasel, D., Rudels, B., Kurz, K., 1988. Outflow of dense water from a Svalbard fjord into the Fram Strait. Deep Sea Research 35, 1143–1150.
Rasmussen, T.L., Thomsen, E., 2009. Stable isotope signals from brines in the Barents Sea: implications for brine formation during the last glaciation. Geology 37, 903–906.
Rasmussen, T.L., Thomsen, E., Slubowska, M.A., Jessen, S., Solheim, A., Koç, N., 2007. Paleoceanographic evolution of the SW Svalbard margin (76°N) since 20,000 ^{14}C yr BP. Quaternary Research 67, 100–114.
Rempfer, J., Stocker, T.F., Joos, F., Dutay, J.-C., Siddall, M., 2011. Modeling Nd isotopes with a coarse resolution ocean circulation model: sensitivities to model parameters and source/sink distributions. Geochimica et Cosmochimica Acta 75, 5927–5950.
Rickli, J., Frank, M., Halliday, A.N., 2009. The hafnium-neodymium isotope composition of Atlantic seawater. Earth and Planetary Science Letters 280, 118–127.
Rudels, B., 1986. The θ-S relations in the northern seas: implications for the deep circulation. Polar Research 4, 133–159.
Rudels, B., Quadfasel, D., 1991. Convection and deep water formation in the Arctic Ocean-Greenland Sea System. Journal of Marine Systems 2, 435–450.
Rudels, B., Jones, E.P., Anderson, L.G., Kattner, G., 1994. On the intermediate depth waters of the Arctic Ocean. In: Johannessen, O.M., Muench, R.D., Overland, J.E. (Eds.), The Role of the Polar Oceans in Shaping the Global Climate. American Geophysical Union, Washington D.C., pp. 33–46.
Rudels, B., Friedrich, H.J., Quadfasel, D., 1999. The arctic circumpolar boundary current. Deep-Sea Research II 46, 1023–1062.
Rudels, B., Meyer, R., Fahrbach, E., Ivanov, V.V., Østerhus, S., Quadfasel, D., 2000. Water mass distribution in Fram Strait and over the Yermak Plateau in summer 1997. Annales Geophysicae 18, 687–705.
Rudels, B., Fahrbach, E., Meincke, J., Budéus, G., Eriksson, P., 2002. The East Greenland Current and its contribution to the Denmark Strait overflow. ICES Journal of Marine Systems 59, 1133–1154.
Rudels, B., Björk, G., Nilsson, J., Winsor, P., Lake, I., Nohr, C., 2005. The interaction between waters from the Arctic Ocean and the Nordic Seas north of Fram Strait and along the East Greenland Current: results from the Arctic Ocean-02 Oden expedition. Journal of Marine Systems 55, 1–30.
Rutberg, R.L., Hemming, S.R., Goldstein, S.L., 2000. Reduced North Atlantic Deep water flux to the glacial Southern Ocean inferred from neodymium isotope ratios. Nature 405, 935–938.
Sarnthein, M., van Kreveld, S., Erlenkeuser, H., Grootes, P.M., Kucera, M., Pflaumann, U., Schulz, M., 2003. Centennial-to-millennial-scale periodicities of Holocene climate and sediment injections off the western Barents shelf, 75°N. Boreas 32, 447–461.
Schauer, U., 1995. The release of brine-enriched shelf water from Storfjord into the Norwegian Sea. Journal of Geophysical Research 100, 16,015–16,028.
Schauer, U., Fahrbach, E., Østerhus, S., Rohardt, G., 2004. Arctic warming through the Fram Strait: oceanic heat transport from 3 years of measurements. Journal of Geophysical Research 109, C06026.
Schaule, B.K., Patterson, C.C., 1981. Lead concentrations in the northeast Pacific: evidence for global anthropogenic perturbations. Earth and Planetary Science Letters 54, 97–116.
Schlichtholz, P., Goszczko, I., 2006. Interannual variability of the Atlantic water layer in the West Spitsbergen Current at 76.5°N in summer 1991–2003. Deep-Sea Research I 53, 608–626.
Schlichtholz, P., Houssais, M.-N., 1999. An inverse modeling study in Fram Strait. Part II: water mass distribution and transports. Deep-Sea Research II 46, 1137–1168.
Schlitzer, R., 2007. Ocean Data View. http://odv.awi.de.
Schoster, F., Behrends, M., Müller, C., Stein, R., Wahsner, M., 2000. Modern river discharge and pathways of supplied material in the Eurasian Arctic Ocean: evidence from mineral assemblages and major and minor element distribution. International Journal of Earth Sciences 89, 486–495.
Sharma, M., Basu, A.R., Nesterenko, G.V., 1992. Temporal Sr-, Nd- and Pb-isotopic variations in the Siberian flood basalts: implications for the plume-source characteristics. Earth and Planetary Science Letters 113, 365–381.
Spielhagen, R.F., Werner, K., Aagaard Sørensen, S., Zamelczyk, K., Kandiano, E., Budéus, G., Husum, K., Marchitto, T.M., Hald, M., 2011. Enhanced modern heat transfer to the Arctic by warm Atlantic Water. Science 331, 450–453.
Steiger, R.H., Jäger, E., 1977. Subcommission on geochronology: convention on the use of decay constants in geo- and cosmochronology. Earth and Planetary Science Letters 36, 359–362.
Stein, R., Dittmers, K., Fahl, K., Kraus, M., Matthiessen, J., Niessen, F., Pirrung, M., Polyakova, Ye., Schoster, F., Steinke, T., Fütterer, D.K., 2004. Arctic (paleo) river discharge and environmental change: evidence from the Holocene Kara Sea sedimentary record. Quaternary Science Reviews 23, 1485–1511.
Stumpf, R., Frank, M., Schönfeld, J., Haley, B.A., 2010. Late Quaternary variability of Mediterranean outflow water from radiogenic Nd and Pb isotopes. Quaternary Science Reviews 29, 2462–2472.
Svendsen, J.I., Mangerud, J., 1997. Holocene glacial and climatic variations on Spitsbergen, Svalbard. The Holocene 7, 45–57.
Swift, J.H., Koltermann, K.P., 1988. The origin of Norwegian sea deep water. Journal of Geophysical Research 93, 3563–3569.
Tachikawa, K., Jeandel, C., Roy-Barman, M., 1999. A new approach to the Nd residence time in the ocean: the role of atmospheric inputs. Earth and Planetary Science Letters 170, 433–446.
Tanaka, T., Togashi, S., Kamioka, H., Amakawa, H., Kagami, H., Hamamoto, T., Yuhara, M., Orihashi, Y., Yoneda, S., Shimizu, H., Kunimaru, T., Takahashi, K., Yanagi, T., Nakano, T., Fujimaki, H., Shinjo, R., Asahara, Y., Tamimizu, M., Dragusanu, C., 2000. JNdi-1: a neodymium isotopic reference in consistency with LaJolla neodymium. Chemical Geology 168, 279–281.
Tütken, T., Eisenhauer, A., Wiegand, B., Hansen, B.T., 2002. Glacial-interglacial cycles in Sr and Nd isotopic composition of Arctic marine sediments triggered by the Svalbard/Barents Sea ice sheet. Marine Geology 182, 351–372.
van de Flierdt, T., Frank, M., 2010. Neodymium isotopes in paleoceanography. Quaternary Science Reviews 29, 2439–2441.
van de Flierdt, T., Robinson, L.F., Adkins, J.F., Hemming, S.R., 2006. Temporal stability of the neodymium isotope signature of the Holocene to glacial North Atlantic. Paleoceanography 21, PA4102.
Véron, A.J., Church, T.M., 1997. Use of stable lead isotopes and trace metals to characterize air mass sources into the eastern North Atlantic. Journal of Geophysical Research 102, 28,049–28,058.
Vinje, T., 2001. Anomalies and trends of sea ice extent and atmospheric circulation in the Nordic seas during the period 1864–1998. Journal of Climate 14, 255–267.
Volkmann, R., 2000. Planktic foraminifer ecology and stable isotope geochemistry in the Arctic Ocean: implications from water column and sediment surface studies for quantitative reconstructions of oceanic parameters. Berichte zur Polarforschung 361, 1–128.
Wanner, H., Beer, J., Bütikofer, J., Crowley, T.J., Cubasch, U., Flückiger, J., Goosse, H., Grosjean, M., Joos, F., Kaplan, J.O., Küttel, M., Müller, S.A., Prentice, I.C., Solomina, O., Stocker, T.F., Tarasov, P., Wagner, M., Widmann, M., 2008. Mid- to Late Holocene climate change: an overview. Quaternary Science Reviews 27, 1791–1828.
Werner, K., Spielhagen, R.F., Bauch, D., Hass, H.C., Kandiano, E., Zamelczyk, K., 2011. Atlantic water advection to the eastern Fram Strait – multiproxy evidence for late Holocene variability. Palaeogeography, Palaeoclimatology, Palaeoecology 308, 264–276.

Please cite this article in press as: Werner, K., et al., Neoglacial change in deep water exchange and increase of sea-ice transport through eastern Fram Strait: evidence from radiogenic isotopes, Quaternary Science Reviews (2013), http://dx.doi.org/10.1016/j.quascirev.2013.06.015

Werner, K., Spielhagen, R.F., Hass, H.C., Bauch, D., Kandiano, E., 2013. Atlantic water advection versus sea ice advances in the eastern Fram Strait during the last 9 ka: Multiproxy evidence for a two-phase Holocene. Paleoceanography 28. http://dx.doi.org/10.1002/palo.20028.

Winter, B.L., Johnson, C.M., Clark, D.L., 1997. Strontium, neodymium, and lead isotope variations of authigenic and silicate sediment components from the Late Cenozoic Arctic Ocean: Implications for sediment provenance and the source of trace metals in seawater. Geochimica et Cosmochimica Acta 61, 4181–4200.

Zimmermann, B., Porcelli, D., Frank, M., Andersson, P.S., Baskaran, M., Lee, D.-C., Halliday, A.N., 2009. Hafnium isotopes in Arctic Ocean water. Geochimica et Cosmochimica Acta 73, 3218–3233.

Please cite this article in press as: Werner, K., et al., Neoglacial change in deep water exchange and increase of sea-ice transport through eastern Fram Strait: evidence from radiogenic isotopes, Quaternary Science Reviews (2013), http://dx.doi.org/10.1016/j.quascirev.2013.06.015